DEVELOPMENT OF A CONCRETE MECHANICAL AND THERMAL PROPERTIES DATABASE FOR PAVEMENT MECHANISTIC-EMPIRICAL INPUT

by

CHANDLER BANKS

(Under the Direction of S. Sonny Kim)

ABSTRACT

State highway agencies (SHAs) in the United States have been moving towards using the Mechanistic-Empirical Pavement Design Guide (MEPDG), which deploys mechanistic and mathematical principles to analyze the material behaviors. For the smooth transition to this updated pavement design approach for rigid pavement design, SHAs have been developing a statewide database of concrete mixture properties to select appropriate input variables and levels for rigid pavement designs. The key mechanical and thermal inputs for rigid pavement design in MEPDG are compressive strength (f'c), modulus of elasticity (Ec), modulus of rupture (MOR), coefficient of thermal expansion (CTE), portland cement concrete (PCC) heat capacity, thermal conductivity, and ultimate shrinkage. This study investigates the effects of thermal properties of concrete mixtures on the performance of rigid pavement. Thermal properties were further investigated using machine learning (ML) algorithms to understand the concrete mixture inputs' impacts.

INDEX WORDS: Pavement ME, concrete materials properties database, thermal properties, sensitivity analysis, machine learning

DEVELOPMENT OF A CONCRETE MECHANICAL AND THERMAL PROPERTIES DATABASE FOR PAVEMENT MECHANISTIC-EMPIRICAL INPUT

by

CHANDLER BANKS

B.S., The University of Georgia, 2019

A Thesis Submitted to the Graduate Faculty of The University of Georgia in Partial Fulfillment of the Requirements for the Degree

MASTER OF SCIENCE

ATHENS, GEORGIA

2020

DEVELOPMENT OF A CONCRETE MECHANICAL AND THERMAL PROPERTIES DATABASE FOR PAVEMENT MECHANISTIC-EMPIRICAL INPUT

by

CHANDLER BANKS

Major Professor:	S. Sonny Kim
Committee:	Mi G. Chorzepa
	Stephan A. Durham
	Jidong J. Yang

Electronic Version Approved:

Ron Walcott
Vice Provost for Graduate Education and Dean of the Graduate School
The University of Georgia
December 2020

ACKNOWLEDGEMENT

The author would like to acknowledge everyone that has played a part in the development of this research. Dr. S. Sonny Kim provided insight and guidance throughout this project serving as a mentor to the author. Committee members Dr. Mi Geum Chorzepa, Dr. Stephan A. Durham, and Dr. Jidong Yang all played vital roles and provided helpful input throughout this project. The author would also like to extend a special thanks to Davis Wing, Alex Blankenship, and Jacob Townsend for their assistance in the batching of the concrete mixtures. On behalf of the author and the University of Georgia, special thanks are owed to the Georgia Department of Transportation for providing the opportunity and funding required for this project.

Table of Contents

List of Tables

List of Figures

1.0 INTRODUCTION

Many design agencies, including Georgia's Department of Transportation (GDOT), rely on 1972, 1981, and 1993 *AASHTO Guide for Design of Pavement Structures* for pavement designs. These design guides were developed by the American Association of State and Highway Transportation Officials (AASHTO) using empirical testing, which requires data collection from the observation of trends and failures through experimentation. This use of empirical testing can be traced back to its use by AASHTO in the 1960s.

As material science continues to develop, research is being performed to explore more precise design approaches. The next step in the design outline can be found in a more mechanistic approach. The mechanistic approach offers insight into the material properties and allows developers to predict performance instead of waiting for an observed failure. This new method offers potential in optimizing the design process. The Mechanistic-Empirical Pavement Design Guide (MEPDG) integrates this mechanistic understanding of the material properties with the established empirical equations.

GDOT is preparing to administer the MEPDG approach in future pavement design projects. For a successful implementation of this mechanistic approach, GDOT requires a material properties database. This thesis seeks to add concrete thermal properties to the recently developed concrete mechanical properties database to provide reliable rigid pavement design using MEPDG. This database will help perform accurate level 1, 2, and 3 designs in Pavement ME software. The thermal properties required to complete a rigid pavement structure in Pavement ME software can be found in Table 1 under the category listed as thermal along with other key input values**.**

Table 1. Thermal Property Inputs Required at Design Levels 1, 2, and 3

Category	Level 1	Level 2	Level 3
PCC	Poisson's Ratio		
	Thickness (in)		
	Unit Weight (pcf)		
Thermal	PCC coefficient of thermal expansion (in/in/deg F x 10^-6)		
	PCC heat capacity (BTU/lb-deg F)		
	PCC thermal conductivity (BTU/hr-ft-deg F)		
Mix	Aggregate type		
	Cementitious material content (lb/yd^3)		
	Cement type		
	Water to cement ratio		
	Curing method		
	Reversible shrinkage (%)		
	PCC zero-stress temperature (deg F)		
	Time to develop 50% of ultimate shrinkage (days)		
	Ultimate shrinkage (microstrain)		
PCC Strength and Modulus	Modulus of rupture (psi) at days: 7, 14, 28, 90	Compressive strength (psi) at days: 7, 14, 28, 90	28-Day PCC modulus of rupture (psi) or compressive strength (psi)
	Elastic Modulus (psi) at days: 7, 14, 28, 90	20-year/28-day estimated compressive strength ratio	28-Day PCC elastic modulus (psi)
	20-year/28-day estimated modulus of rupture and elastic modulus ratios		

These thermal properties will be determined for the 12 GDOT approved mixtures. The mixtures focus on critical mixture characteristics, including cementitious content, water-to-cementitious ratio (w/cm), fly ash content, coarse aggregate type, coarse aggregate volume fraction, and air content. This mixture matrix offers a large diversity in the concrete materials database and allows researchers and engineers to understand the effects of various mechanical and thermal properties important for pavement design.

The thermal properties relevance is explored in this thesis through level three sensitivity analyses for a jointed plain concrete pavement (JPCP) structure. The Pavement ME software generated several distresses that the pavement structure may encounter during its lifetime. The sensitivity analyses allowed relationships and trends between the thermal properties and the predicted distresses to be formed. ML techniques were also applied to determine the factors that impacted the thermal properties the most. Determining each thermal property's relevance in the software's prediction of distresses and the factors that affect those properties will offer benefits when using MEPDG to design rigid pavement structures.

2.0 BACKGROUND IN GEORGIA

2.1 Background of MEPDG in Georgia

GDOT currently relies on the *1981 AASHTO Interim Guide for Design of Pavement Structures* for their rigid pavement design. The organization has funded several research projects in hopes of transitioning to the use of AASHTOWare's *Pavement ME Design* software (Pavement ME), which implements the MEPDG approach. Previous research projects have provided GDOT with existing dynamic modulus and asphalt binder databases for Georgia asphalt mixtures. These projects include RP 12-07 "Measurements of Dynamic and Resilient Moduli of Roadway Test Sites," GDOT project RP 14-12 "Effects of Reclaimed Asphalt Pavement (RAP) Contents and Sources on Dynamic Modulus (E*) and Fatigue Performance of Asphalt Mixtures in Georgia," GDOT project RP 16-19 "Development of MEPDG Input Database for Asphalt Mixtures," and GDOT project 17-18 "Development of Innovative & Effective Training Modules and Methods for Pavement Designers for Rapid Deployment and Continuous Operation of MEPDG." These projects, along with a symposium that demonstrated a step-by-step rigid and flexible pavement design for GDOT engineers using the MEPDG approach, all strive to implement this advanced design approach into Georgia's Department of Transportation. GDOT also sponsored a project that hoped to calibrate the MEPDG global distress transfer functions to match local Georgia conditions (Quintus et al., 2015). The study used Georgia Long-Term Pavement Performance (LTPP) and non-LTPP to determine the Georgia calibration coefficients and assist in the determination of the smoothness and distress calculations using the MEPDG software (Quintus et al., 2015).

These sections are comprised of GDOT design practices and materials specifications. The LTPP sections could be related to specific features for jointed plain concrete pavements (JPCP) including, joint spacing, dowels, shoulders, and base types. Out of the eleven LTPP sections, only

one contained an asphalt concrete (AC) base interlayer, and only two of the LTPP sections were comprised of the continuously reinforced concrete pavements (CRCP). Non-LTPP roadway segments were also selected to fill the cells in the sampling matrix. This would balance the factorial and include segments that exhibited higher distress levels than the typical threshold values or design criteria used by GDOT. These sight locations are displayed in Figure 1.

Figure 1. Rigid Pavement Sites (Quintus et al., 2015)

The LTPP and non-LTPP sites allowed a successful estimation of the bias and precision of the MEPDG rigid and flexible pavement transfer functions that allowed the prediction of the performance indicators (roughness and distress) of the department's pavements. Once this project was completed, Applied Research Associates (ARA) developed *The GDOT Pavement ME Design User Input Guide* (ARA, 2015). GDOT engineers have used this guide to follow a step-by-step procedure when designing a pavement structure using the Pavement ME software. The input guide contains Georgia-specific values for various properties and information required in the software. *The GDOT Pavement ME Design User Input Guide* has been updated in 2020 (Kim et al., 2020).

2.2 Background of Mechanical Properties in Georgia

GDOT RP 18-03 study, entitled "Development of Concrete Mechanical Properties Database for Pavement Mechanistic-Empirical Input," continued the transition to the MEPDG approach to design rigid pavement in Georgia. The project aimed to develop a concrete mechanical and thermal properties database to assist GDOT engineers in completing level 1, 2, and 3 rigid pavement designs in the Pavement ME software. To assure all mixtures met GDOT standards, twelve previously GDOT approved concrete mixtures were selected. The mixtures were carefully selected with various inputs and aggregate types to create a diverse materials database with a wide application range. The twelve mixtures are displayed in Table 2 and will be the same mixtures used in this study to develop the thermal properties database.

Table 2. Mixture Matrix (Wing, 2018)

Mixture Number	Mixture ID	Cementitious Content	Fly Ash (%)	w/cm	CA Type	CA Fraction	Air Content (%)
1	541/0FA/0.431/11.91G/4.9	541	0	0.431	Granite	11.91	4.9
2	541/0FA/0.524/12.75G/4.0	541	0	0.524	Granite	12.75	4.0
3	595/0FA/0.43/11.4G/6.2	595	0	0.43	Granite	11.4	6.2
4	600/0FA/0.47/11.62G/6.1	600	0	0.47	Granite	11.62	6.1
5	580/12.2FA/0.493/12.54G/4.5	580	12.2	0.493	Granite	12.54	4.5
6	579/19.69FA/0.446/11.67G/5.5	579	19.69	0.446	Granite	11.67	5.5
7	622/26FA/0.422/12.14G/3.1	622	26	0.422	Granite	12.14	3.1
8	605/20.66FA/0.43/12.09D/5.0	605	20.66	0.43	Dolomite	12.09	5.0
9	590/18.64FA/0.438/10.87G/4.9	590	18.64	0.438	Granite	10.87	4.9
10	590/18.64FA/0.439/10.87D/5.9	590	18.64	0.439	Dolomite	10.87	5.9
11	600/20.16FA/0.47/11.42G/3.6	600	20.16	0.47	Granite	11.42	3.6
12	600/20.16FA/0.47/11.42G/4.7	600	20.16	0.47	Granite	11.42	4.7

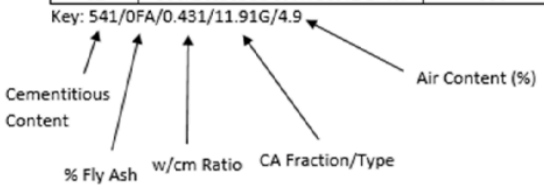

The study provided a laboratory tested value for all of the mechanical properties found in the Pavement ME software, including compressive strength (f'c), Young's modulus, modulus of rupture (MOR), modulus of elasticity (MOE), and ultimate shrinkage. After the experimental data was collected, comparisons were made between varying mixtures to see individual inputs' effects on the mechanical properties. Compressive strength was affected by air content, fly ash

replacement, w/cm, coarse aggregate (CA) type, and CA fraction. The compressive strength was measured at different ages, including 7 days, 14 days, 28 days, and 90 days. A level 1 and 2 design in the Pavement ME program require all four of these values for compressive strength, while a level 3 design only requires a 28-day f'c value or a 28-day MOR value. This study discovered many correlations between the mixture characteristics, mechanical properties, and the Pavement ME software summarized below.

- The fly ash (Class F) admixture did not exhibit a reaction originally, however as the concrete specimen aged, the mixtures containing fly ash continued to produce calcium silicate hydrate (CSH), which allowed for a continued strength development throughout the specimen's lifetime.
- The MOE test results allowed researchers to determine the factors affecting the MOE of concrete mixtures: fly ash content, aggregate type, and w/cm. Higher fly ash content and w/cm result in lower MOE values, while the most impactful factor is the aggregate type. The MOE mixtures using dolomite demonstrated much higher MOE values than similar mixtures containing granite.
- All twelve GDOT approved mixtures displayed an equal or higher Poisson's ratio value than the default of 0.20. Pavement ME will not accurately predict the distresses if the default Poisson's ratio (0.2) is used because the estimated lateral strain is less than the strain the pavement structure actually endures. The Poisson's ratio test results illustrate little interaction with age but a noticeable reaction to the aggregate type.
- Pavement ME software does not use the American Concrete Institute (ACI) empirical equation for estimating MOR values. The equation listed as Equation 1 is typically used to estimate MOR values when laboratory testing cannot occur.

$$\textbf{MOR} = 7.5 * \sqrt{f'c}\ \textbf{(psi)} \qquad \textbf{Equation 1}$$

The software uses a prediction equation labeled Equation 2 when estimating MOR. This prediction equation leads to a higher estimation than the estimation obtained from the ACI equation.

$$\textbf{MOR} = 9.5 * \sqrt{f'c}\ \textbf{(psi)} \qquad \textbf{Equation 2}$$

The laboratory tested MOR values were plotted with both of these estimation equations and were determined to fit very closely to equation 2, the equation used in the Pavement ME software. While this validates the software's use of this equation, it also displays the advantage of having a concrete property database and avoiding this concern. MOR demonstrated an inverse relationship with air content, in which mixtures with higher air contents displayed lower MOR values.

- Ultimate shrinkage was the final mechanical property in this study. The experimental data illustrated a relationship between the w/cm and shrinkage values. Mixtures containing higher w/cm resulted in a larger percentage of differences in the specimen's length. This study recommended additional investigation be performed for ultimate shrinkage and the mixture characteristics affecting this mechanical property.
- Along with the development of the mechanical properties database, the study investigated which of the Pavement ME software's mechanical properties had the most significant impact on rigid pavements. The analyses determined that jointed plain concrete pavement (JPCP) design was sensitive to compressive strength, unit weight, Poisson's ratio, and MOR. Compressive strength and MOR were particularly impactful on the international roughness index (IRI) and percent slabs cracked. In comparison, unit weight and Poisson's ratio played a key role in predicting mean joint faulting. The sensitivity analysis of CRCP

structures confirmed it was only sensitive to MOR and compressive strength with concern to mechanical properties.

2.3 Background of Thermal Properties in Georgia

Kim (2012) conducted GDOT RP 10-04 study to lay the groundwork to help GDOT move towards using MEPDG for rigid pavement design. Through the study, the concrete mixture characteristics that influence the coefficient of thermal expansion (CTE) was investigated. Through the research, a database of CTE values for 68 different mixtures was developed. This data determined the significance of the following variables affecting CTE: coarse aggregate type, coarse aggregate content, fine aggregate type, air content, water-to-cement ratio, fly ash content, and fly ash type. The variety of mixtures contains three coarse aggregate types: limestone, dolomite, and granite, as well as two types of fine aggregates: natural sand (NS) and manufactured sand (MS). The 68 mixtures are displayed in Table 3.

Table 3. Concrete Mixture Design for Concrete Cylinders (Kim, 2012)

CTE No.	**Batch No.**	**Gr. CA** (lb/yd3)	**Dol. CA** (lb/yd3)	**Lim. CA** (lb/yd3)	**MS** (lb/yd3)	**NS** (lb/yd3)	**C-Ash** (lb/yd3)	**F-Ash** (lb/yd3)	**Cement** (lb/yd3)	**Air Content** (%)	**Slump** (in.)
1	1	2100	0	0	950	0	20	0	530	3	2
2	2	2100	0	0	950	0	20	0	530	6	2
3	17	2100	0	0	950	0	160	0	460	3	2
4	18	2100	0	0	950	0	160	0	460	6	2
5	33	2100	0	0	950	0	0	20	530	3	2
6	34	2100	0	0	950	0	0	20	530	6	2
7	49	2100	0	0	950	0	0	160	460	3	2
8	50	2100	0	0	950	0	0	160	460	6	2
9	5	2100	0	0	0	950	20	0	530	3	2
10	6	2100	0	0	0	950	20	0	530	6	2
11	21	2100	0	0	0	950	160	0	460	3	2
12	22	2100	0	0	0	950	160	0	460	6	2
13	37	2100	0	0	0	950	0	20	530	3	2
14	38	2100	0	0	0	950	0	20	530	6	2
15	53	2100	0	0	0	950	0	160	460	3	2
16	54	2100	0	0	0	950	0	160	460	6	2
17	3	1150	0	0	1900	0	20	0	530	3	2
18	4	1150	0	0	1900	0	20	0	530	6	2
19	19	1150	0	0	1900	0	160	0	460	3	2
20	20	1150	0	0	1900	0	160	0	460	6	2
21	35	1150	0	0	1900	0	0	20	530	3	2
22	36	1150	0	0	1900	0	0	20	530	6	2

CTE No.	**Batch No.**	**Gr. CA** (lb/yd3)	**Dol. CA** (lb/yd3)	**Lim. CA** (lb/yd3)	**MS** (lb/yd3)	**NS** (lb/yd3)	**C-Ash** (lb/yd3)	**F-Ash** (lb/yd3)	**Cement** (lb/yd3)	**Air Content** (%)	**Slump** (in.)
23	51	1150	0	0	1900	0	0	160	460	3	2
24	52	1150	0	0	1900	0	0	160	460	6	2
25	7	1150	0	0	0	1900	20	0	530	3	2
26	8	1150	0	0	0	1900	20	0	530	6	2
27	23	1150	0	0	0	1900	160	0	460	3	2
28	24	1150	0	0	0	1900	160	0	460	6	2
29	39	1150	0	0	0	1900	0	20	530	3	2
30	40	1150	0	0	0	1900	0	20	530	6	2
31	55	1150	0	0	0	1900	0	160	460	3	2
32	56	1150	0	0	0	1900	0	160	460	6	2
33	9	0	2100	0	950	0	20	0	530	3	2
34	10	0	2100	0	950	0	20	0	530	6	2
35	25	0	2100	0	950	0	160	0	460	3	2
36	26	0	2100	0	950	0	160	0	460	6	2
37	41	0	2100	0	950	0	0	20	530	3	2
38	42	0	2100	0	950	0	0	20	530	6	2
39	57	0	2100	0	950	0	0	160	460	3	2
40	58	0	2100	0	950	0	0	160	460	6	2
41	13	0	2100	0	0	950	20	0	530	3	2
42	14	0	2100	0	0	950	20	0	530	6	2
43	29	0	2100	0	0	950	160	0	430	3	2
44	30	0	2100	0	0	950	160	0	430	6	2
45	45	0	2100	0	0	950	0	20	530	3	2
46	46	0	2100	0	0	950	0	20	530	6	2
47	61	0	2100	0	0	950	0	160	460	3	2
48	62	0	2100	0	0	950	0	160	460	6	2
49	11	0	1150	0	1900	0	20	0	530	3	2
50	12	0	1150	0	1900	0	20	0	530	6	2
51	27	0	1150	0	1900	0	160	0	460	3	2
52	28	0	1150	0	1900	0	160	0	460	6	2
53	43	0	1150	0	1900	0	0	20	530	3	2
54	44	0	1150	0	1900	0	0	20	530	6	2
55	59	0	1150	0	1900	0	0	160	460	3	2
56	60	0	1150	0	1900	0	0	160	460	6	2
57	15	0	1150	0	0	1900	20	0	530	3	2
58	16	0	1150	0	0	1900	20	0	530	6	2
59	31	0	1150	0	0	1900	160	0	460	3	2
60	32	0	1150	0	0	1900	160	0	460	6	2
61	47	0	1150	0	0	1900	0	20	530	3	2
62	48	0	1150	0	0	1900	0	20	530	6	2
63	63	0	1150	0	0	1900	0	160	460	3	2
64	64	0	1150	0	0	1900	0	160	460	6	2
65	65	0	0	2100	950	0	160	0	460	3	2
66	66	0	0	1150	1900	0	160	0	460	3	2
67	67	0	0	2100	0	950	160	0	460	3	2
68	68	0	0	1150	0	1900	160	0	460	3	2

In GDOT RP 10-04 study, Kim (2012) used materials locally available in Georgia. The used aggregate had varying nominal maximum aggregate size (NMAS), which were ¾" for granite and ½" for dolomite. The gradations performed for the differing aggregate types followed the American Society for Testing and Materials (ASTM) C33 specifications. The location, the physical properties, and primary aggregate classification for the aggregates selected are listed in Table 4.

Table 4. Aggregate Physical Properties (Kim, 2012)

Aggregate	Coarse Aggregate Location in GA	Aggregate Group	Absorption (%)	Magnesium Sulfate Soundness Loss, %	Specific Gravity		
					Bulk	S.S.D	APP
Granite	Columbus	II	0.62	0.8	2.677	2.693	2.722
Dolomite	Adairsville	I	0.64	0.5	2.805	2.823	2.857

Kim (2012) concluded that the most crucial elements affecting CTE values are coarse aggregate type, stone volume, and sand type. This assessment seems logical when determining the relationship between heat and these various mixtures when the aggregate content of such mixtures can be as high as 80% of the mixture volume. The measured average CTE of mixtures that contained dolomite and granite are located in Table 5.

Table 5. Aggregate Type Effect on CTE (Kim, 2012)

Coarse Aggregate	Average CTE	Standard Deviation
Granite	4.751 με /°F (8.552 με /°C)	0.4 με /°F (0.72 με /°C)
Dolomite	4.847 με /°F (8.725 με /°C)	0.35 με /°F (0.63 με /°C)

Kim (2012) found that dolomite mixtures exhibit a relatively higher CTE value than granite mixtures. Along with aggregate types, stone volume and sand type played a large role in affecting the concrete specimens' CTE values. Mixtures that used natural sand (NS) resulted in higher CTE

values compared to the mixtures containing manufactured sand (MS). The aggregate proportion effects on CTE values are presented in Table 6.

Table 6. Aggregate Proportion Effect on CTE (Kim, 2012)

Coarse Aggregate	Stone Volume	Sand Type	Average CTE		Standard Deviation	
			με /°F	με /°C	με /°F	με /°C
Granite	High	MS	4.384	7.891	0.115	0.208
		NS	4.906	8.831	0.168	0.303
	Low	MS	4.442	7.996	0.119	0.214
		NS	5.272	9.490	0.184	0.332
Dolomite	High	MS	4.623	8.322	0.126	0.228
		NS	4.982	8.967	0.152	0.273
	Low	MS	4.534	8.162	0.120	0.216
		NS	5.318	9.573	0.131	0.235

When examining the effects of mineral admixtures on CTE values of concrete specimens, class C-fly ash mixtures contained significantly higher values than class F-fly ash mixtures. However, outside of the fly ash type, the study did not establish an obvious relationship between the mixtures with or without the mineral admixture. The study recommended that further testing occurred on various quarries throughout Georgia to establish a more developed CTE database (Kim, 2012). The outcomes of mixtures that contained different fly ash types are illustrated in Table 7.

Table 7. Fly Ash Type Effect on CTE (Kim, 2012)

Coarse Aggregate	Volume	Sand Type	Average CTE (με/°F)				Average CTE (με/°C)			
			C-Fly Ash		F-Fly Ash		C-Fly Ash		F-Fly Ash	
			Low	High	Low	High	Low	High	Low	High
Granite	High	MS	4.384	4.481	4.454	4.216	7.892	8.065	8.017	7.590
		NS	5.046	4.990	4.895	4.694	9.082	8.982	8.811	8.448
	Low	MS	4.439	4.593	4.454	4.284	7.990	8.268	8.017	7.710
		NS	5.426	5.429	5.218	5.017	9.766	9.772	9.392	9.030
Dolomite	High	MS	4.735	4.681	4.636	4.440	8.523	8.426	8.345	7.993
		NS	5.128	5.085	4.938	4.776	9.231	9.153	8.889	8.596
	Low	MS	4.640	4.598	4.549	4.351	8.351	8.277	8.189	7.831
		NS	5.456	5.393	5.277	5.147	9.821	9.707	9.499	9.264

Kim et al. (2015) investigated the effect of age and materials on CTE of concrete paving mixtures at 28 and 120 days (Kim et al., 2015). Multiple mixtures were examined for this study;

these mixtures contained different aggregate types and underwent scanning electron microscopy, observing these varying mixtures' microstructures. The study hoped the understanding of these microstructures would offer insight into the further understanding of the relationship between volume change in concrete and the formation of microcracks. Kim et al. (2015) used statistical analyses shown in Table 8 to illustrate the CTE values of the specimens measured at 120 days were significantly lower than the values measured at 28 days. This study proved that age does affect the coefficient of thermal expansion values in concrete specimens.

Table 8. Statistics of CTE at 28 and 120 days (Kim et al. 2015)

	CTE ($\mu\varepsilon$/°C) measured at	
Descriptive statistics	28 days	120 days
Min.	8.05	7.48
Max.	9.87	9.79
Median	8.83	8.39
Mean	8.88	8.50
Stdev	0.66	0.70

Kim et al. (2015) found that CTE values of concrete mixtures were largely affected by the specimen's materials, validating previous CTE research in Georgia. The average CTE value of mixtures containing limestone was drastically lower than that of mixtures containing dolomite or granite. This study found a relationship between the aggregates and effects of age on CTE results, particularly that mixtures containing granite had significantly higher CTE reduction with time than mixtures composed of dolomite.

3.0 LITERATURE REVIEW

3.1 Thermal Inputs

Thermal properties provide key insight into understanding and predicting the performance of a concrete mixture. The distinctive thermal attributes among each portland cement concrete (PCC) mixture produce a key understanding of heat flow inside a material (Shin & Kodide, 2012). Pavement ME software contains three thermal inputs when using a PCC layer in a design; those inputs are coefficient of thermal expansion (CTE), thermal conductivity, and heat capacity. All three of these thermal properties play a role in the flow of heat through the pavement structure and influence the moisture profile and temperature distribution in these structures. A study performed by Chintakunta (2007) at Iowa State University explored the sensitivity of thermal properties of pavement materials using MEPDG. This study performed sensitivity analyses to help identify the general behavior of the thermal properties and flaws in the software's MEPDG models, the results of this research are listed below.

- JPCP structures demonstrated expected results based on established pavement engineering knowledge concerning cracking and faulting models. The transverse cracking was proven to be sensitive to both thermal conductivity and CTE, and the faulting model was similarly sensitive to thermal conductivity and CTE in addition to dowels and surface shortwave absorptivity (SSA). International roughness index (IRI) exhibited sensitivity for CTE, SSA, and thermal conductivity. These analyses proved the obvious correlations between thermal properties and common pavement distresses.
- CRCP structures demonstrated expected results based on established pavement engineering knowledge concerning punchout and IRI models. CTE proved to be the most critical input for IRI and punchouts, while crack spacing, ultimate shrinkage strain, SSA, thermal conductivity, and climate also played a role in CRCP structures' punchouts.

- Cracking in JPCP structures are most affected by thermal conductivity, heat capacity, SSA, and CTE.
- Punchouts in CRCP structures are most affected by thermal conductivity, ultimate shrinkage, heat capacity, SSA, and CTE.
- In hot mix asphalt (HMA) pavements, heat capacity and thermal conductivity did not affect any distresses in MEPDG.

3.1.1 Coefficient of Thermal Expansion

CTE is considered the change in unit length per degree of temperature change. This thermal property is a key factor in PCC's study and design due to its direct relationship to temperature-related pavement deformations throughout the mixture's lifetime (Kim, 2012). Recent research and sensitivity analysis have proved that CTE is a delicate input in the Mechanistic-Empirical Pavement Design Guide (MEPDG). CTE has been proven to play a key role in the slab stresses because of its influential role in corner deflections, joint faulting, initial temperature-induced movements, pavement smoothness, and saw cut timing (ARA, 2004).

A study performed by Mallela et al. (2005) examined the significance of CTE for concrete in rigid pavement design proved, along with these slab stresses and thermal deformations, CTE demonstrates an effect on JPCP through joint opening and closing as well as crack opening and closing in CRCP. The CTE values of a concrete mixture can be traced to the concrete's component materials. Aggregate type is the most influential factor regarding this thermal property. A reasonable explanation can be stated in terms of volume; aggregates form roughly 70 to 80% of the volume of a concrete mixture and would, in return, be the most influential factor. Along with aggregate type, CTE is affected by the hardened paste content, cement content, water-cement ratio, porosity degree of hydration (age) of paste, and humidity. This thermal property is regarded as a critical property due to the many impacts it has on a concrete structure. Regarding JPCP

performance, CTE affects transverse cracking (caused by top-down and bottom-up fatigue cracking), joint faulting, and smoothness. Simultaneously, the effect of CTE on CRCP is primarily concerned with crack width, punchouts, and smoothness.

CTE can cause early-age or premature random cracking if restraint forces resist too much longitudinal slab movement created by high CTE. High curling stresses allow for more mid-panel transverse and longitudinal cracking and an increase in faulting due to a greater loss of slab support during construction. This faulting results in increased joint opening and greater corner deflections from curling. The extreme opening and closing of joints create joint sealant failures and allow for joint spalling, and the crack width is particularly impactful on CRCP structures design life with regards to crack load transfer efficiency and punchouts (Mallela et al., 2005).

3.1.2 Thermal Conductivity and Heat Capacity

Thermal Conductivity is the ratio of heat flux to the temperature gradient. In a designated sample thickness, this ratio indicates the uniform flow of heat from one side of the sample to the other. Heat transfer in concrete is similar to that of metals due to its porous and heterogeneous nature as a solid material. Multiple factors, including aggregate type, temperature, and moisture of local environment, cement paste content, coarse and fine aggregate, along with porosity and admixtures, affect the thermal conductivity of concrete (Kodide, 2010). Thermal Conductivity can be calculated using the formula listed as Equation 3.

$$K = (\Delta Q * x) / (\Delta t * A * \Delta T) \qquad \textbf{Equation 3}$$

K = Thermal Conductivity of the material

ΔQ = Change in heat energy between two points

x = Distance between two points

Δt = Heat flow for a given change in time

A = Area of the object in which heat flow is measured

ΔT = Change in temperature that produced a change in heat flow

Table 9. Heat Capacity and Thermal Conductivity Units (Kodide, 2010)

Parameters	S.I Unit	Conversion Factor	English Unit
Thermal Conductivity	1 W/m-K	0.5779	Btu/ft-h-ºF
Heat Capacity	1 J/m^3-K	1.49 x 10^{-5}	Btu/ft^3-ºF

Thermal conductivity can be measured in several ways, but this research is primarily focused on the transient heat line approach utilized in the ASTM D5334-14 test method. A line source of heat will be applied by an electrical probe inserted into the concrete specimen. The thermal conductivity will be determined by measuring the rate at which the concrete specimen's temperature changes in response to the applied heat.

The study performed by Kodide (2010) at Louisiana State University used various concrete mixtures that contained different aggregates to identify the relevance that aggregate has on the thermal conductivity of concrete. The mixtures can be found in Table 10.

Table 10. Concrete Mixture Designs for Thermal Conductivity (Kodide, U. 2010)

Mixtures	Unit	K65 (0.451)	K20 (0.547)	K80 (0.451)	G65 (0.451)	M65 (0.451)
Holcim Type II (GP) Portland Cement	lbs/yd³	475	475	475	475	475
Sand, A133 TXI Dennis Mills	lbs/yd³	1,171	2,551	637	1,131	1,149
Kentucky Limestone, AB29 Martin Marietta	lbs/yd³	2,104	654	2,612	-	-
Gravel, A133 TXI Dennis Mills	lbs/yd³	-	-	-	2,027	-
Mexican Limestone, AA36	lbs/yd³	-	-	-	-	2,071
% by volume Fine Aggregate	%	36.2	80	20	35.0	35.7
% by volume Coarse Aggregate	%	63.8	20	80	65.0	64.3
Water	lbs/yd³	214	260	214	214	214
Water Cement Ratio		0.451	0.547	0.451	0.451	0.451
Admixture (Daravair 1400)	Dosage (oz/100ct)	0.50	0.50	0.50	0.50	0.50
Admixture (WRDA 35)	Dosage (oz/100ct)	3.50	10.0	2.0	6.40	20.00
ASTM C 1064 Air Temperature	°F	68.5	75.3	70.0	69.0	71.2
ASTM C 1064 Concrete Temperature	°F	72.0	78.0	70.9	73.5	74.6
ASTM C 143 Slump	inches	0.25	0.0	0.25	1.50	1.25
ASTM C 231 Pressure Air Content	%	7.00	3.50	3.60	6.30	4.00
ASTM C 138 Unit Weight	lbs/ft³	144.4	143.2	148.8	140.0	149.2
Specific gravity	-	2.69	2.69	2.69	2.53	2.62
Water absorption	%	1.0	1.0	1.0	2.2	3.5

(K: Kentucky limestone; G: Gravel; M: Mexican limestone)

The aggregates were determined to play a major role in the thermal conductivity of the concrete mixtures. The mixtures containing the gravel aggregate had a much higher thermal conductivity than the mixtures containing limestone. This study also demonstrated a linear relationship between the increase in thermal conductivity and moisture content. Moisture has proven to be a crucial factor affecting thermal conductivity in concrete specimens. Kodide (2010) also investigated the relevance of thermal conductivity on a pavement section using a MEPDG analysis. The study found that while there was little interaction between thermal conductivity and mean joint faulting, thermal conductivity did affect transverse cracking. A higher thermal conductivity value reduces the temperature difference from the top to the bottom of the pavement structure, which caused a reduction in predicted distresses.

Another study concluded that a concrete specimen's porosity had a dramatic influence on the thermal conductivity (dos Santos, W.N. 2003). The material porosity levels allow the water to have a large impact due to moisture storage in the specimen. Concrete specimens with high porosities allow for larger water absorption, directly related to a higher thermal conductivity value (dos Santos, W.N. 2003).

Bentz et al. (2011) from the National Institute of Standards and Technology conducted a study exploring the relationship between density and thermal conductivity in concrete mixtures. Varying amounts of fly ash were substituted for the cement to produce a lower density concrete mixture. The study demonstrated a positive correlation between density and thermal conductivity in the tested specimens. Bentz et al. (2011) concluded that a larger fly ash replacement percentage resulted in a lower density, producing lower thermal conductivity. The study went on to discover that lower thermal conductivity values result in lower thermal diffusivity. A lower thermal

diffusivity allows concrete to serve as a thermal buffer and be less affected by environmental temperature changes.

Heat Capacity (C_p) is also a thermal property required for the MEPDG approach. It is simply the ability of a mixture to store its internal energy while being subjected to temperature change and remaining in the same physical state. Therefore, it is the actual amount of heat energy required to change a unit mass's temperature by a single degree (Chintakunta 2007). The heat capacity of a substance depends mainly on the mass and size of a mixture's constituents. Heat capacity differs from thermal conductivity in this manner. The thermal conductivity value for coarse and fine aggregates is the same; however, the fine aggregate's heat capacity would be much lower than that of coarse aggregate due to its reliance on mass and size. For concrete mixtures, the water content and porosity will also play a role in heat capacity (Kodide, U. 2010). Heat capacity demonstrated an inverse relationship with a linear decrease in heat capacity as the moisture increases.

Fly ash has been proven to have little impact on specific heat capacity test results in concrete mixtures. Benz et al. (2011) concluded that water content was the key factor affecting concrete's specific heat capacity. Table 11 illustrates the varying specific heat capacity values for materials in a concrete mixture. This data illustrates water's specific heat value of 4.18 J/(g K) is significantly higher than other materials and provides an explanation for water playing the largest role in specific heat capacity values for concrete mixtures.

Table 11. Specific Heat Values of Concrete Mixture Materials (Bentz et al. 2011)

Material	Specific Heat Capacity (J/(g K))
Water	4.18
Cement (Type IP)	0.76
Fly Ash (Class F)	0.72
Limestone Sand	0.76

3.2 Pavement ME Software Concrete Property Input Relevance

Determining the relevance of concrete property inputs in Pavement ME software demonstrates the importance of developing a concrete materials database. Using the *AASHTO Mechanistic-Empirical Pavement Design Guide-A Manual of Practice* (2008), a series of flowcharts illustrate the software's decision-making process in pavement performance predictions. The flowcharts display mean transverse joint faulting, smoothness (predicted IRI), transverse slab cracking (bottom-up and top-down) for JPCP structures, as well as punchouts for CRCP structures. A key to understanding the various roles of inputs and calculations in the mechanistic-empirical design software is displayed in Figure 2.

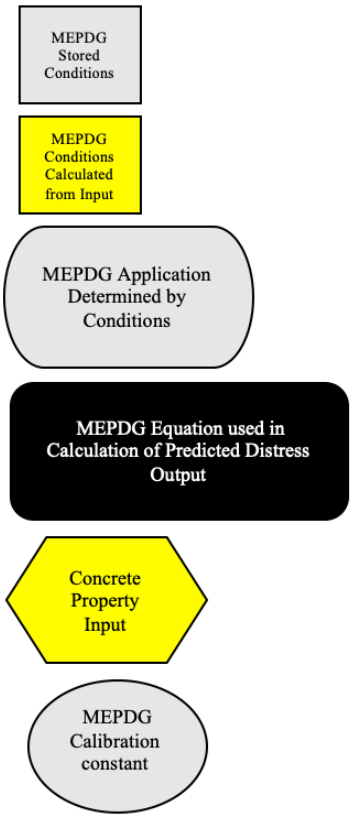

Figure 2. Flowchart Key

The flowcharts serve as a visual aid in understanding the major equations, inputs, and processes used in the Pavement ME software to predict performance indicators. The flowcharts do not include every step in the software's decision-making process, but the arrows can be followed to show the process and interconnection between the major inputs and applications. Other factors, including neural nets, local calibrations, and input dependent functions, are excluded. The CRCP punchouts flowchart is listed in Figure 3. In the punchout prediction model, it is important to recognize that CTE directly impacts the load transfer efficiency (LTE). LTE is the ratio of deflection of the unloaded side to the joint's loaded side and a larger LTE results in a greater reduction of stresses and deflections in the concrete slab. A manual of practice summarizes the prediction of punchouts in CRCP are due to the loss of crack LTE, erosion along the edge of the

slab throughout the structure's design life, and the effects of permanent and transitory moisture and temperature gradients.

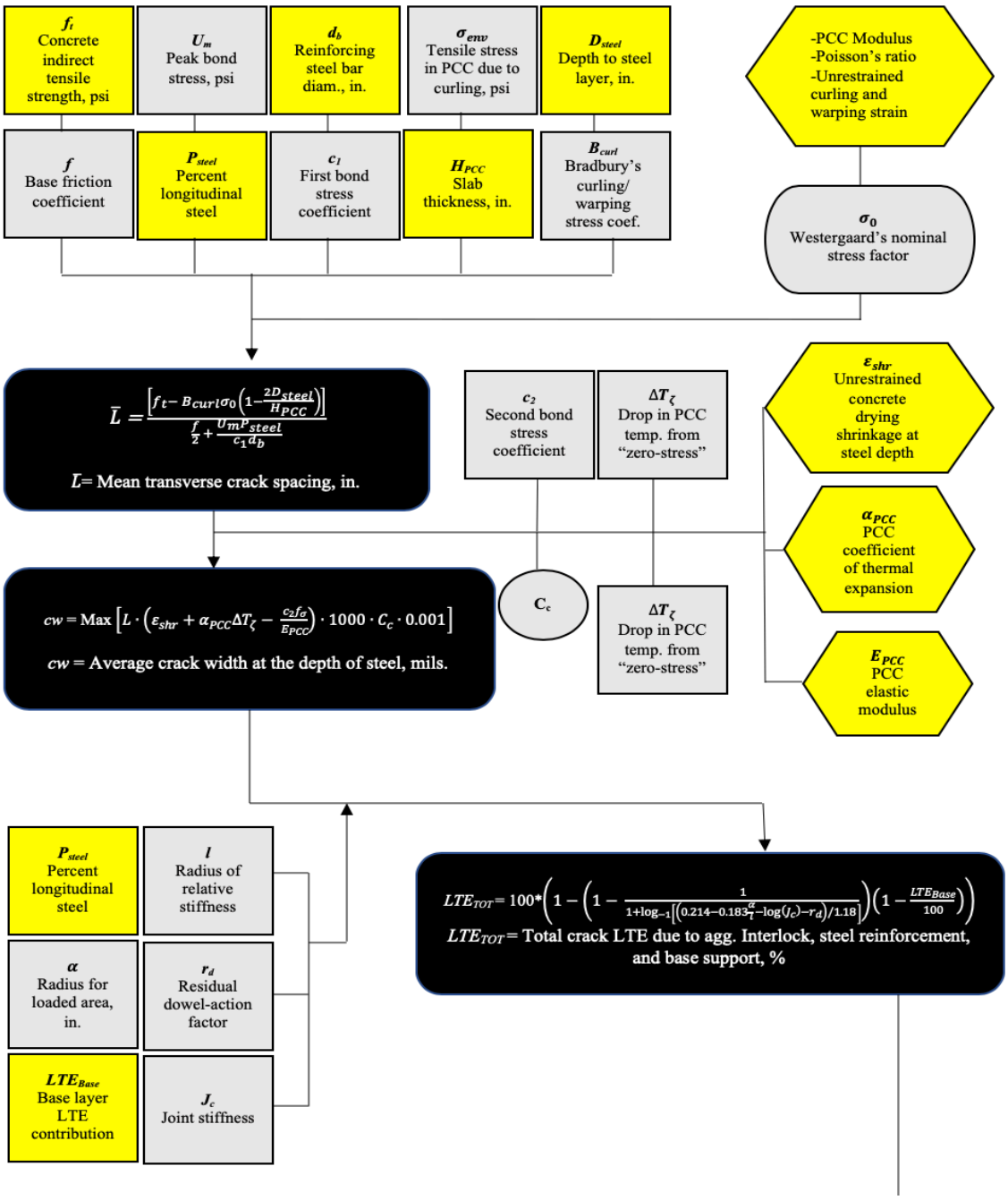

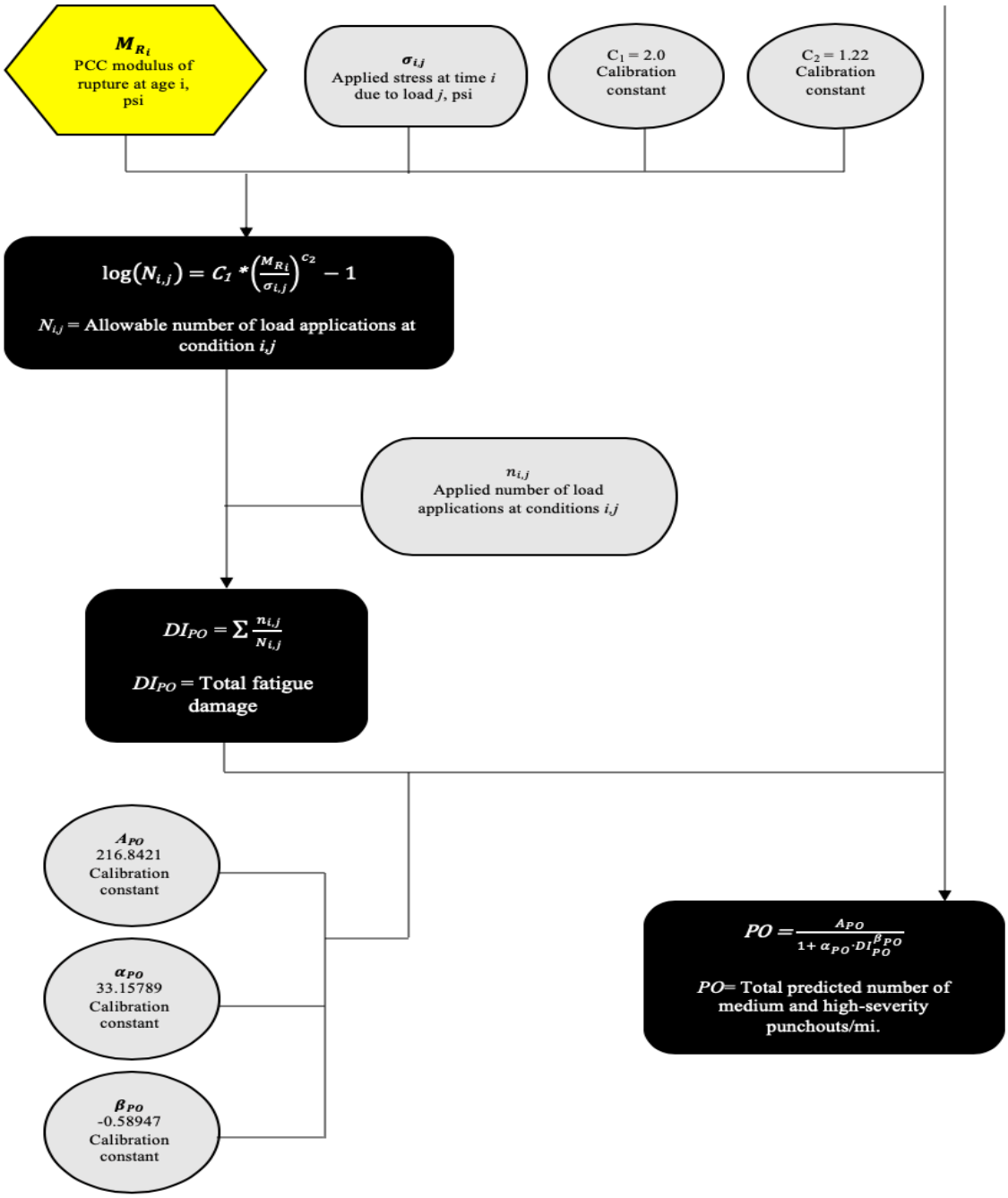

Figure 3. CRCP Punchouts Flowchart

Both bottom-up and top-down modes of JPCP transverse slab cracking are considered in Figure 4. Both modes of cracking can occur in all JPCP structures subjected to normal service conditions; however, both forms of cracking will not occur simultaneously.

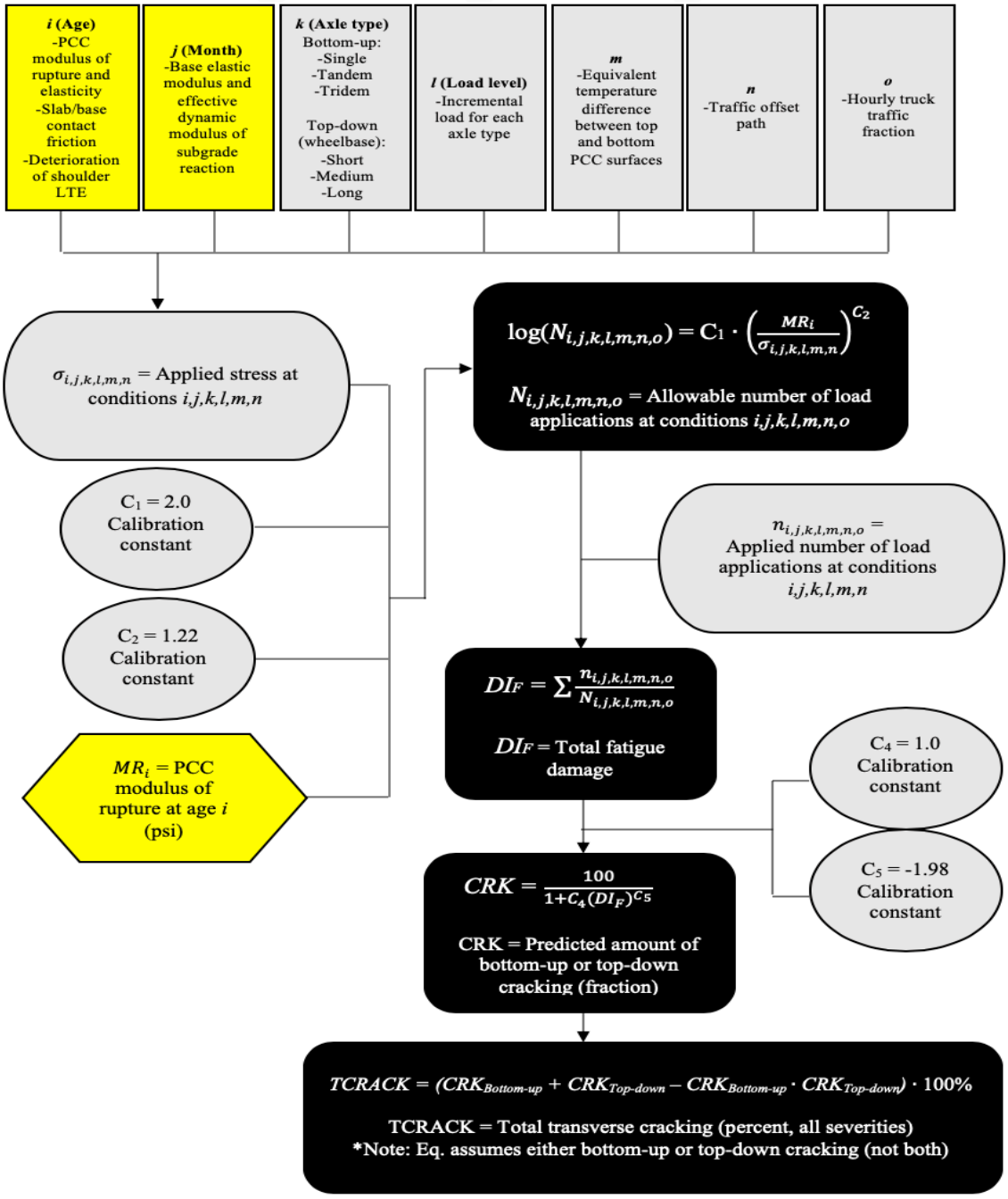

Figure 4. JPCP Transverse Slab Cracking (Bottom-Up and Top-Down) Flowchart

The permanent curl/warp effective temperature difference input in Pavement ME software contains a built-in temperature gradient at the set time of the structure, an effective gradient of moisture warping, and the effect of long-term creep of the slab and settlement into the base.

The smoothness performance indicator flowchart for JPCP structures in AASHTOWare Pavement ME Design is displayed in Figure 5. This distress is predicted as a function of the initial as-constructed profile of the pavement, traffic effects on foundation movements, and any change in the longitudinal profile throughout the structure's service life. The IRI model was calibrated and validated using the LTPP field data discussed earlier to eliminate any variable from climate or field conditions.

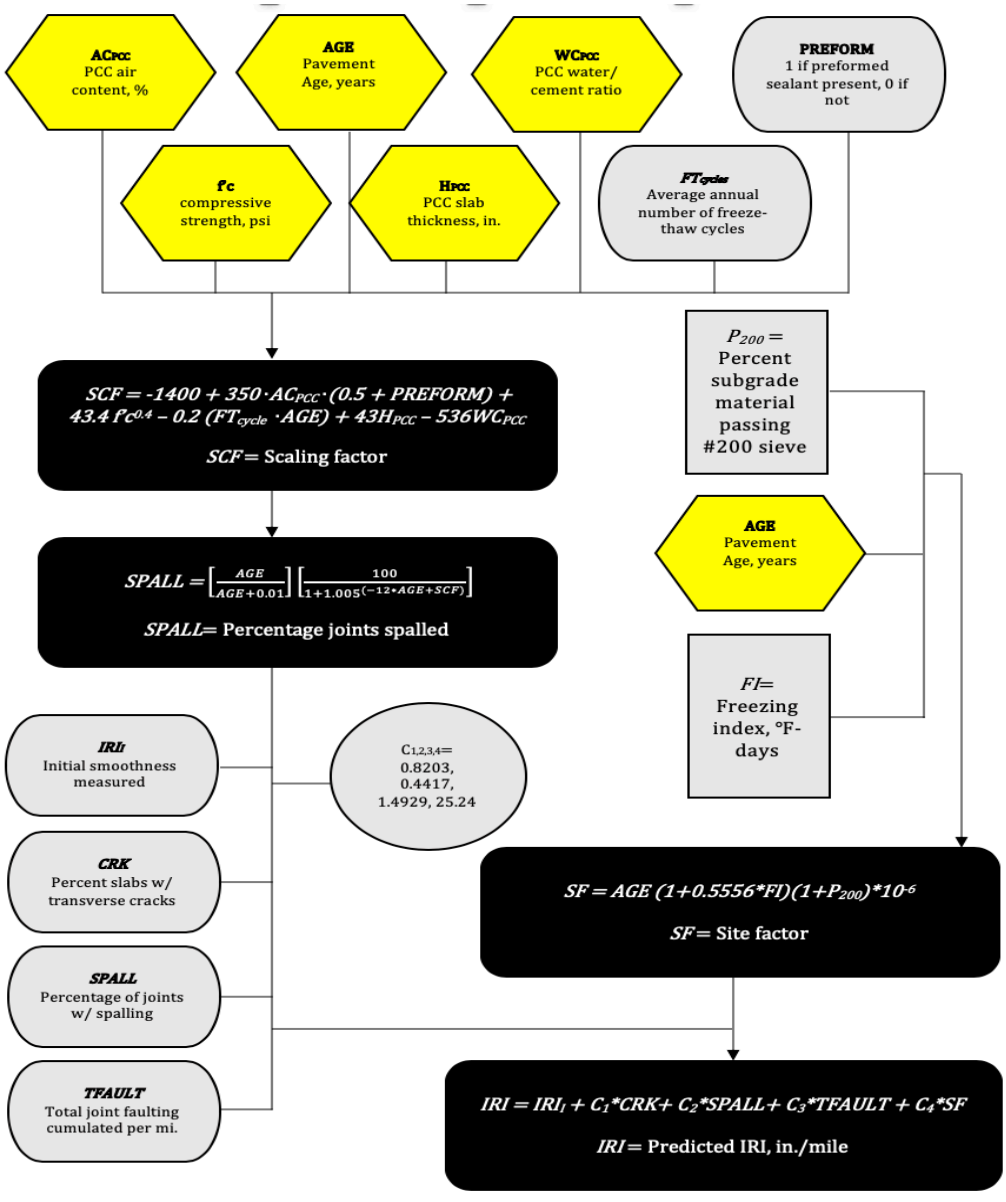

Figure 5. JPCP Smoothness (Predicted IRI) Flowchart

Figure 6 explores the decision-making process of the Pavement ME software in determining mean transverse joint faulting. This performance indicator is critical in determining the ride quality a JPCP structure will provide throughout its service life. This pavement distress is a combination of repeated applications of heavy axle loads, poor load transfer across the joint, free moisture beneath the PCC slab, erosion of the supporting base/subbase, subgrade, or shoulder base material, and upward curling of the slab.

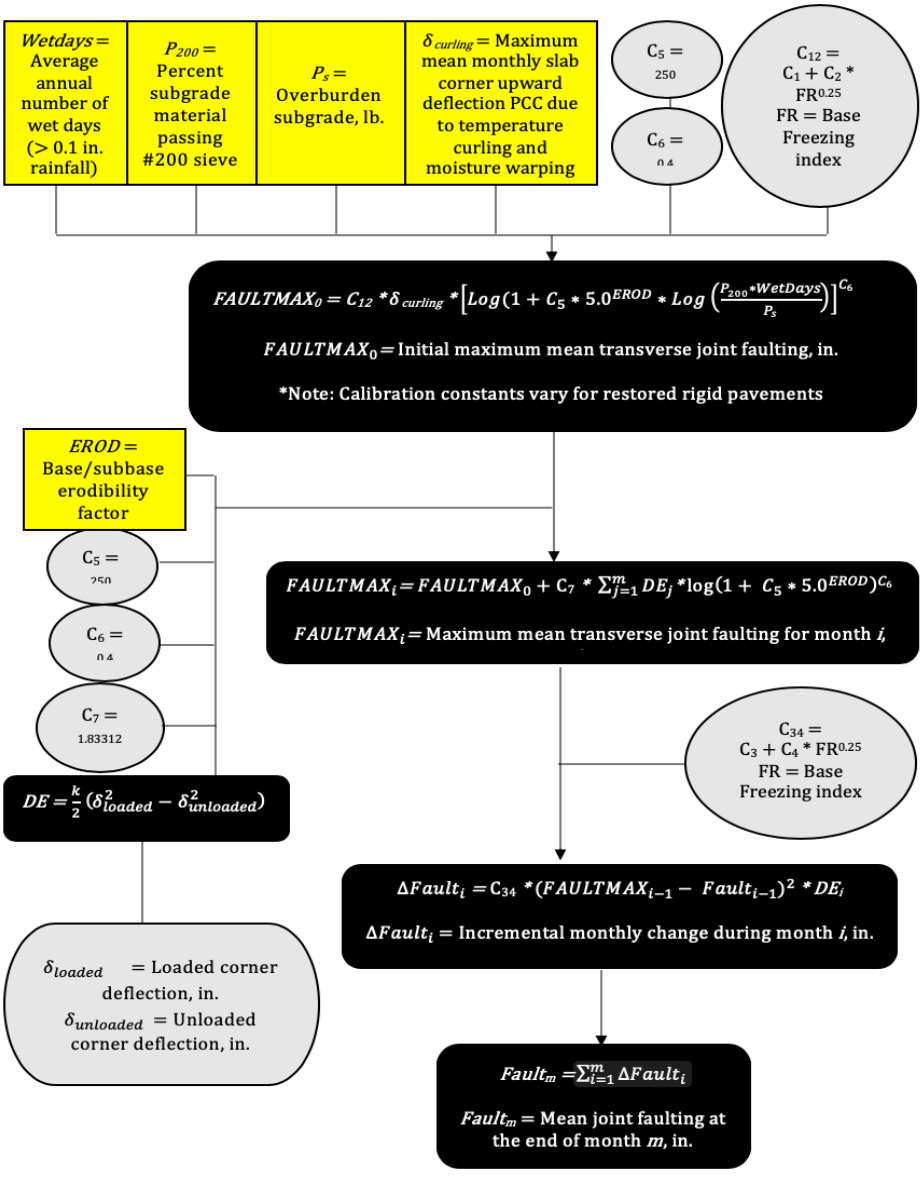

Figure 6. JPCP Mean Transverse Joint Faulting Flowchart

4.0 PROBLEM STATEMENT

Design standards for rigid pavement structures were founded on the principle of empirical testing. While these design procedures have proven successful, they do not utilize the mechanistic-empirical design approach's benefits. As material science continues to advance, highway design agencies will move toward this new approach that continues to prove its worth. The most commonly used design method implementing this new approach is *AASHTOWare Pavement ME Design Software* (2011), which is generally referred to as the Mechanistic-Empirical Pavement Design Guide (MEPDG). However, even with access to these innovative design guides, some pavement design departments and agencies still have not fully transitioned to this new approach.

GDOT has been proactive in its transition to the MEPDG approach for rigid pavement design. In 2010, GDOT initiated the RP 10-04 project to establish the initial step to move forward to MEPDG rigid pavement design using single quarry material. In 2018, the concrete mechanical properties database was expanded using 12 GDOT approved mixtures through RP 18-03 study. This database creation was a large step forward in the implementation of MEPDG in Georgia.

This thesis seeks to complete the concrete materials database by providing accurate and lab-tested values for the AASHTOWare Pavement ME Software's thermal properties. These thermal properties include the coefficient of thermal expansion, thermal conductivity, and heat capacity. With the completion of this concrete materials database, GDOT engineers can complete level 1, 2, and 3 designs confidently. Along with the completion of the concrete materials database, this study aims to use statistical analysis and a machine learning approach to provide an in-depth understanding of concrete mixtures inputs and characteristics and their role in the mechanical and thermal properties of the concrete.

5.0 MATERIALS

This research's main objective is to provide GDOT with a comprehensive concrete materials database for rigid pavement design using the MEPDG approach. To prepare the most functional collection of experimental data, a variety of materials were selected across the state of Georgia. With a large selection of mixtures containing various materials, GDOT will perform level 1, 2, and 3 designs for a wide range of future projects. All of the materials and their respective properties will be included in this section to provide a deeper understanding of the concrete mixture's individual inputs.

5.1 Aggregates

The aggregates used in this project were selected from five different quarries. Four of the quarries were selected for coarse aggregates. The four different quarries were selected based on their location, one quarry from North Georgia (location 1), two quarries from Metro-Atlanta (locations 2 and 3), and one quarry from Middle/South Georgia (location 4). There are no quarries located south of Macon. Therefore, any projects located below the quarries selected will use aggregate from these quarries or quarries with similar locations. The diverse selection of quarries will provide GDOT with an adequate selection of different coarse aggregates when completing new projects throughout Georgia. The fifth quarry location was selected for fine aggregate. This quarry provided the research team with natural sand (NS) for the concrete mixtures. The use of NS is practical in Georgia projects due to its proximity and abundance and offering better finishing qualities compared to manufactured sand (MS). NS has been proven to provide higher thermal property test values than MS. These higher thermal property values will assure that similar mixtures containing MS will not underestimate these properties when using a mechanistic-design approach. Since NS has fairly similar properties, the team concluded that one quarry would be

sufficient to represent fine aggregates commonly used in Georgia projects. The quarry information is displayed in Table 12 and the column labeled "Quarry Number" can be referenced in Figure 7.

Table 12. Quarry Information

Location	Quarry Number	Company	Quarry ID	Aggregate Type	Mixtures Using Quarry
North	1	Vulcan	Adairsville 120C	Dolomite, Group I	8,10
Metro	2	Vulcan	Kennesaw 46C	Meta-Quartz Diorite, Group II	3,4
	3	Vulcan	Stockbridge 50C	Granite Gneiss, Group II	5,6,7,9
Middle/South	4	Martin Marietta	Ruby 054C	Gneiss/Amphibolite, Group II	1,2,11,12
Middle/South	5	Atlanta Sand	Roberta 002F	Alluvial/Marine Sand	1-12

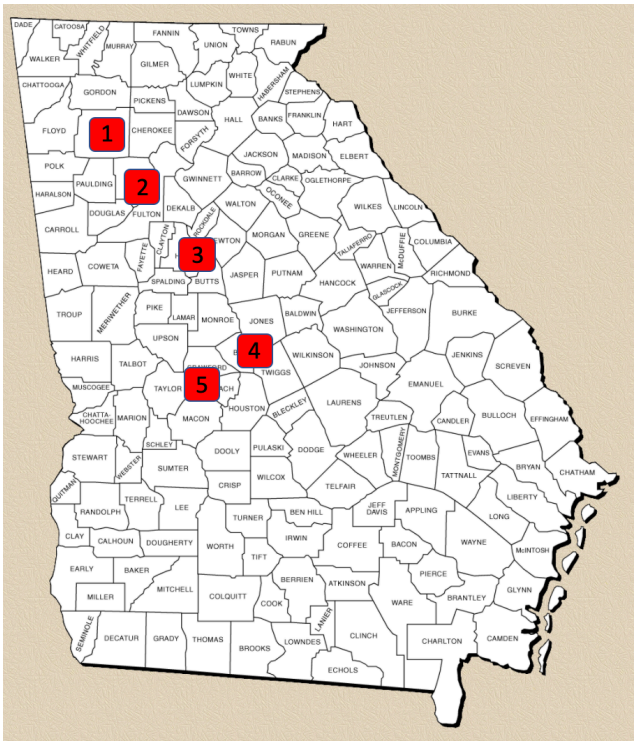

Figure 7. Quarry Locations

Coarse aggregate specifications are discussed in GDOT Section 800, and the size specifications are provided in Table 13. All of the coarse aggregates in this study uses the #57 stone gradation.

Table 13. GDOT Section 800 Coarse Aggregate Specifications

SIZE NO	NOMINAL SIZE SQUARE OPENINGS		AMOUNTS FINER THAN EACH LABORATORY SIEVE (SQUARE OPENINGS). %, BY WEIGHT										
	(1)	mm	2 ½"	2"	1 ½"	1"	¾"	½"	3/8"	No. 4	No. 8	No- 16	No. 50
			63 mm	50 mm	37.5mm	25 mm	19 mm	12.5 mm	9.5 mm	4.75 mm	2.36mm	1.18 mm	300 µm
3	2-1	50 - 25	100	90-100	35-70	00-15	-----	00-5	----	-----	-----	-----	-----
357	2-No. 4	50 - 4.75	100	95-100	-----	35-70	-----	10-30	----	00-5	-----	-----	-----
4	1 ½ -3/4	37.5 - 19	-----	100	90-100	20-55	00-15	-----	00-5	-----	-----	-----	-----
467	1 ½- No. 4	37.5 - 4.75	-----	100	95-100	-----	35-70	-----	10-30	00-5	-----	-----	-----
5	1-1/2	25 – 12.5	-----	-----	100	90-100	20-55	00-10	00-5	-----	-----	-----	-----
56	1-3/8	25 – 9.5	-----	-----	100	90-100	40-75	15-35	00-15	00-5	-----	-----	-----
57	1-No. 4	25 – 4.75	-----	-----	100	95-100	-----	25-60	-----	00-10	00-5	-----	-----
6	¾-3/8	19 – 9.5	-----	-----	-----	100	90-100	20-55	00-15	00-5	-----	-----	-----
67	¾-No. 4	19 – 4.75	-----	-----	-----	100	90-100	-----	20-55	00-10	00-5	-----	-----
68	¾-No. 8	19 –2.36	-----	-----	-----	100	90-100	-----	30-65	05-25	00-10	0-5	-----
7	½-No. 4	12.5 – 4.75	-----	-----	-----	-----	100	90-100	40-70	00-15	00-5	-----	-----
78	½-No. 8	12.5 – 2.36	-----	-----	-----	-----	100	90-100	40-75	05-25	00-10	0-5	-----
8	3/8-No. 8	9.5 – 2.36	-----	-----	-----	-----	-----	100	85-100	10-40	0-10	0-5	-----
89	3/8-No. 16	9.5 – 1.18	-----	-----	-----	-----	-----	100	90-100	20-55	0-15	0-10	0-5
9	No. 4-No. 16	4.75 – 1.18	-----	-----	-----	-----	-----	-----	100	85-100	10-40	0-10	0-5

In the previous study conducted by Wing (2018), the coarse aggregates all displayed a very similar gradation, seen in Figure 8. Despite the similar gradations, the coarse aggregates had differing absorption capacities and specific gravity values. A summary of the values can be found in Table 14, and the complete material sheets for the quarries are located in Appendix A.

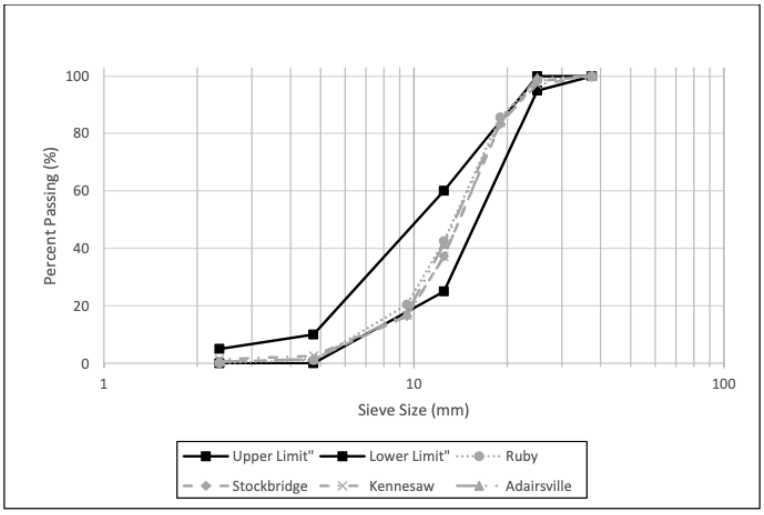

Figure 8. Coarse Aggregate Gradation (Wing, 2018)

Table 14. Coarse Aggregate's Specific Gravity and Absorption Capacity (QPL)

Quarry Number	Quarry ID	Absorption Capacity (%)	Specific Gravity (SSD)
1	Adairsville 120C	0.08	2.847
2	Kennesaw 46C	0.65	2.763
3	Stockbridge 50C	0.60	2.625
4	Ruby 054C	0.50	2.732

Fine aggregate specifications are discussed in GDOT Section 801. Table 15 serves as a reference to this section, where the fine aggregate being used in this project is described as natural concrete sand with size no. 10 NS. The material sheet for detailed information regarding quarry No. 5 can be found in Appendix A.

Table 15. GDOT Section 801 Fine Aggregate Specifications (QPL)

Size No.	Description	Total Percent by Weight Passing Each Sieve					
		3/ 8 in (9.5 mm)	No. 4 (4.75 mm)	No. 16 (1.18 mm)	No. 50 (300 µm)	No. 100 (150 µm)	No. 200 (75 µm)
10 NS	Natural concrete sand	100	95-100	45-95	8-30	1-10	0-3
20 NS	Natural mortar sand	100	100	90-100	15-50	0-15	0-5
10 SM	Standard manufactured concrete sand	100	95-100	45-95	8-30	1-10	0-4
10 FM	Fine manufactured concrete sand	100	95-100	45-95	15-42	8-22	3-9

5.2 Cement

Type I/II cement was used in concrete mixtures for this study. The cement's physical analysis can be found in Table 16 and the chemical analysis in Table 17, and a full material certification report in Appendix A. The type I/II cement has a specific gravity of 3.13.

Table 16. Physical Analysis of Cement

Physical Analysis		
Item	**Spec Limit**	**Test Result**
Air Content of mortar (%) (C185)	12 max	7
Blaine Fineness (m^2/kg) (C204)	260	396
0.325 (%) (C430)	-	97.2
Autoclave expansion (%) (C151)	0.80 max	0.08
Compressive Strength (psi,[Mpa]) (C109)		
1 day	-	2090 [14.4]
3 days	1740 [12.0] min	3910 [27.0]
7 days	2760 [19.0] min	4892 [33.7]
28 days	-	6420 [44.3]
Time of setting (minutes)		
Vicat Initial (C191)	45-375	101
Heat of Hydration (kj/kg) (C1702) 3 days	-	298
Mortar Bar Expansion (%) (C1038)	0.020 max	0.003
Specific Gravity (C188)	-	3.13

Table 17. Chemical Analysis of Cement

Chemical Analysis		
Item	**Spec Limit**	**Test Result**
Rapid Method, X-Ray (C114)		
SiO2(%)	-	19.8
Al2O3 (%)	-	4.7
Fe2O3 (%)	-	3.2
CaO (%)	-	62.8
MgO (%)	6.0 max	3.0
SO3 (%)	3.0 max	3.0
Loss on ignition (%)	3.5 max	2.7
Insoluable Residue (%)	1.5 max	0.51
CO2 (%)	-	1.7
Limestone (%)	5.0 max	2.3
CaCO3 in Limestone (%)	70 min	99
Inorganic Process addition (Baghouse Dust)	5.0 max	2.0
Adjusted Potential Phase Composition (C150)		
C3S (%)	-	54
C2S (%)	-	15
C3A (%)	-	7
C4AF (%)	-	10
NaEq	0.6 max	0.36

5.3 Admixtures

Only two admixtures were used in this study, one mineral (Class F fly ash) and one chemical (air-entraining admixture). Admixtures have proven to affect concretes properties positively and are a common practice. Due to admixtures' presence in many pavement design projects, the study aims to provide GDOT employees with mixtures where admixtures are present.

5.3.1 Fly Ash

Fly ash (Class F) was the only mineral admixture involved in this research. Boral MC donated the fly ash from Plant Bowen in Cartersville, GA. The physical and chemical properties are listed in Table 18 and 19 respectfully, with a full material testing datasheet in Appendix A. A Class F fly ash was selected for this research due to its common usage in Georgia for rigid pavement construction. The admixture has a specific gravity of 2.47.

Table 18. Physical Analysis of Fly Ash

Physical Analysis		
Item	**Result**	**AASHTO Limit**
Fineness, % retained on a 45-µm sieve	14.48%	34 max
Strength Activity Index		
7 day, % of control	82%	75 min
28 day, % of control	82%	75 min
Water Requirement, % control	98%	105 max
Autoclave Soundness	0.01%	0.8 max
Specific Gravity	2.47	-

Table 19. Chemical Analysis of Fly Ash

Chemical Analysis		
Item	**Result (%)**	**AASHTO Limit**
SiO2	47.49	-
AL2O3	21.3	-
Fe2O3	18.08	-
Sum(SiO2+Al2O3+Fe2O3)	86.87	70 min
SO3	2.07	5.0 max
CaO	4.26	-
MgO	1.19	-
Na2O	0.99	-
K2O	2.32	-
Na2O+0.658K2O	2.52	-
Moisture	0.14	3.0 max
Loss on Ignition	1.23	5.0 max
Available Alkalies, as Na2Oe	1.03	1.5 max

5.3.2 Air Entraining Admixture

Air entraining admixture (AEA) is the only chemical admixture selected in this study. This admixture helps contractors better control the concretes air levels and is commonly known for improving concretes workability. The AEA dosage varied from mixture to mixture, primarily because of its interaction with the mineral admixture fly ash. Mixtures that embody fly ash require a higher AEA dosage to attain the typical 3.0 – 6.0 % GDOT target air content as a mixture without fly ash. This study used Darex II AEA for its concrete mixtures; this admixture complies with ASTM C260 admixture specifications. Darex recommends this admixture be added to the concrete mixture at approximately ½ to 5 fl oz/100 lbs (30 to 320 mL/100 kg) of cement.

6.0 EXPERIMENTAL DESIGN

6.1 Design Plan

This study plans to complete the concrete materials database by adding the thermal properties required to complete a MEPDG design for future rigid pavement projects in Georgia. Twelve GDOT approved mixtures were batched and tested for the crucial remaining thermal properties, including CTE, thermal conductivity, and ultimate shrinkage. The batched concrete was tested for fresh concrete properties, including slump, temperature, air content, and unit weight. Batching and testing for this research were conducted at the UGA-STRENGTH (STRuctural ENGineering Testing Hub) Laboratory. These various mixtures have been previously tested for mechanical properties, including compressive strength (f'c), modulus of elasticity (MOE), Poisson's ratio, modulus of rupture (MOR), and ultimate shrinkage (Wing, 2018). This study also implemented a machine learning algorithm to demonstrate the important role each thermal property input plays in the Pavement ME software's performance prediction indicators. Also, level 3 sensitivity analyses were completed to demonstrate the thermal properties' critical impacts on MEPDG design.

6.2 Concrete Mixture Testing Matrix

In a previous study performed by Wing (2018), a concrete testing matrix, located in Table 20, was developed using twelve previously used GDOT mixtures. The mixtures were composed of varying amounts of cementitious content, fly ash replacement percentage, water-to-cementitious ratio (w/cm), coarse aggregate type, coarse aggregate volume fraction, and air content. Through material proportioning and selection, the concrete mixtures contain a variety of inputs and results, which offer a broad database for GDOT employees using the database to perform MEPDG designs and see the role that the varying mixture characteristics and properties play in the Pavement ME

software. In Table 20, the variable that is being isolated can be found in the last column labeled "Variable of Concern" and is also marked in with an asterisk symbol (*).

Table 20. Concrete Mixture Matrix

Mixture Number	Cement Content (lbs/yd^3)	Fly Ash (%)	w/cm	CA Type	CA Fraction	Air Content (%)	Variable of Concern
1	541*	0	0.42*	Granite	12.75	5.00	Low Cement/ w/c ratio change
2	541*	0	0.51*	Granite	12.75	5.00	
3	580*	0	0.42*	Granite	12.75	5.00	High Cement/ w/c ratio change
4	580*	0	0.51*	Granite	12.75	5.00	
5	580	15*	0.42	Granite*	12.75*	5.00	Fly Ash/ Granite Content
6	580	20*	0.42	Granite*	12.75*	5.00	
7	580	25*	0.42	Granite*	12.75*	5.00	
8	580	20	0.42	Dolomite*	12.75*	5.00	Dolomite Content
9	580	20*	0.42	Granite*	10.00*	5.00	Fly Ash/ Granite Content
10	580	20	0.42	Dolomite*	10.00*	5.00	Dolomite Content
11	580	20	0.42	Granite	12.75	3.00*	Air Content
12	580	20	0.42	Granite	12.75	6.50*	

6.3 Experimental Procedures

6.3.1 Material Preparation

This project followed the guidelines provided in *ASTM C192: Standard Practice for Making and Curing Concrete Test Specimens in the Laboratory* when batching the concrete to provide accurate and trusted experimental data. This American Society for Testing and Materials

(ASTM) standard provides information regarding the preparation of the materials, the mixing of the concrete, curing procedures, and specimen preparation. First, the preparation of the molds for the test specimens took place. The reusable molds were lightly coated with a suitable nonreactive release agent. Before mixing, the properly stored materials were weighed in five-gallon buckets and were brought to room temperature ranging from 68 to 86ºF (20 to 30ºC). The weights of the aggregate were determined after the moisture content had been calculated according to *ASTM C566: Standard Test Method or Total Evaporable Moisture Content of Aggregate by Drying* with separate consideration of size fraction between the coarse and fine aggregates.

6.3.2 Concrete Mixing

After the materials were properly prepared, the mixing procedure was ready to take place. Before the drum mixer began rotation, the coarse aggregate and some of the mixing water that contains the solution of the liquid AEA admixture are added to the mixer. The mixer then begins rotation, and fine aggregate, water, fly ash, and cement are distributed into the mixer. When adding fly ash, the pozzolan admixture is handled in the same manner as the cement. When all materials are placed in the mixer, the concrete is mixed for three minutes, then undergoes a three-minute resting period and is concluded with a two-minute mixing period. The mixed concrete was then placed into a damp wheelbarrow remixed by a shovel or trowel until it looks uniform and ready to be placed into the testing molds.

6.3.3 Curing of Concrete

After the concrete is properly mixed and placed in the test specimen mold, it hardened for approximately 24 ± 8 hours before it was removed. To prevent evaporation from the freshly mixed concrete, the specimens were covered with a nonabsorptive, durable impervious plastic. Once the specimens were ready to be removed from the molds, they were placed in a storage tank following

the *ASTM C511-13: Standard Specification for Mixing Rooms, Moist Cabinets, Moist Rooms, and Water Storage Tanks Used in the Testing of Hydraulic Cements and Concretes*. All of the specimens were moist cured at 73.5 ± 3.5ºF (23.0 ± 2.0ºC) until the moment of testing. The tank contained a calcium hydroxide (CaOH) powder to prevent the leaching of calcium from specimens, and a circulatory pump was used to ensure this powder and the temperature of the tank were evenly distributed amongst all specimens.

6.3.4 Concrete Testing Procedures

The concrete mixtures were subjected to two different types of testing after the concrete was mixed. The first type of testing occurred immediately after the removal of the concrete from the drum mixer. This testing occurred to determine the fresh concrete properties and allows researchers to understand the concrete's behavior and simple quality assurance. The next type of testing occurs after the concrete is placed in its selected mold and properly cured for a specified amount of time. The specifications on these hardened concrete specimens vary from testing property to testing property. The hardened concrete properties of concern in the study include CTE, thermal conductivity, and ultimate shrinkage. ASTM or AASHTO provides strict guidelines, and these test standards for the fresh concrete properties and the hardened concrete properties can be found in Tables 21 and 22, respectively.

Table 21. Fresh Concrete Testing Standards

Fresh Concrete Property	Test Standard ID
Temperature	AASHTO T309/ASTM C1064
Slump	AASHTO T119/ASTM C143
Unit Weight	AASHTO T121/ASTM C138
Pressure Meter Air Content	AASHTO T152/ASTM C231

Table 22. Hardened Concrete Testing Standards

Concrete Property Test	Test Standard ID	Time Period
Modulus of Rupture	ASTM C78/ AASHTO T23	28 and 90 days
Density and Void Content	ASTM C1754	28 days
Ultimate Shrinkage	AASHTO T160/ ASTM C157	0, 3, 7, 14, 28, 35, 42, 49, 56, 63, 70, 77
Coefficient of Thermal Expansion	AASHTO TP 60	After 28 days
Thermal Conductivity	ASTM D5334-14	After 28 days

CTE and thermal conductivity test specimens were both 4 x 8" (101.6 x 203.2 mm) cylinders. Before CTE testing, the specimens were cut to a length of 7 $\pm$ 0.1" (177.8 $\pm$ 2.5 mm) to satisfy testing requirements. Large 6 x 6 x 22" (152.4 x 152.4 x 558.8 mm) beams were used for the modulus of rupture (MOR) testing. For ultimate shrinkage testing 4 x 4 x 10" (101.6 x 101.6 x 254 mm) beams were used.

The MOR test results were used to validate and compare concrete mixtures used for thermal testing to the previous study performed by Wing (2018). Two large MOR beams were tested for each GDOT approved mixture, one at 28 days and one at 90 days.

CTE testing was performed on two concrete cylinders subjected to a uniform increase from 50 to 122°F (10 to 50ºC) and a decrease of 50 to 122°F (10 to 50ºC) temperature. The change in length of the specimen in millimeters was measured as the heating and cooling cycles occurred, and the average change in length of the concrete specimen per unit change in temperature was the resulting CTE.

A line source method was used for thermal conductivity testing. The probe issued a known current and voltage, and the temperature increase of the specimen concerning time was measured. After the probe quit providing heat to the specimen, the temperature decay of the was measured. The thermal conductivity was calculated by analyzing the time and temperature relationship

between the heat and cooling cycles. The twelve concrete mixtures each had six concrete cylinders that underwent testing after the 28-day curing period. The testing focused on the impact of density, moisture, and air content on thermal conductivity in concrete. Each concrete mixture had an extra cylinder tested for density following the ASTM C1754 test method after the 28-day curing period.

The six cylinders were tested in three different conditions, two cylinders per condition. The first condition was oven dry. This condition was obtained by placing the concrete specimens in an oven at a temperature of 100 ± 5 °F (38± 3°C) for 24 ±1 hour. After this 24-hour time period, the specimen was removed, and the mass was determined; this process continued in 24-hour increments until the two subsequent mass determinations had a difference of less than 0.5%. The second condition was referred to as a normal condition. This condition was obtained by placing two cylinders into a controlled environmental chamber that maintained a temperature of 73± 3 °F (23± 2°C) and relative humidity of 50 ± 4%. The specimens remained in this chamber for a 24-hour period to ensure homogeneous temperature and moisture throughout the specimen. After this 24-hour period, the specimens were tested. The final condition was saturated. After 28-days, the concrete specimens were moved from the moisture-curing tank to a water tank inside the environmental chamber for a 24-hour period. At the end of this 24-hour period, the saturated specimens were then tested. Each specimen underwent ten individual tests, and any outliers defined by ASTM E178 were removed before averaging the test results.

Ultimate shrinkage test results were the average of the three beam specimens. The specimens were stored in the same environmental chamber that maintained a temperature of 73± 3 °F (23± 2°C) and relative humidity of 50 ± 4%. For the first 28 days, the shrinkage specimens were wet cured; after they reached the 28-day mark, they were removed from the water storage tanks and left to air dry.

7.0 EXPERIMENTAL RESULTS AND PAVEMENT ME ANALYSIS

7.1 Concrete Mixtures

Regarding Table 20, the past study conducted by Wing (2018) selected previously used GDOT mixtures that isolated the same variables of concern. The research group searched for concrete mixtures that had been previously used and implemented by the department of transportation that matched similar desired mixture characteristics. The mixtures from previous projects can be found in Table 23 with mixture inputs and the project number.

Table 23. GDOT Approved Mixtures

Mixture Number	Cementitious Content (lbs/yd^3)	Fly Ash (%)	w/cm	CA Type	CA Fraction	Air Content (%)	GDOT Project ID
1	541	0	0.431	Granite	11.91	3.0-6.5	IM-185-1(326)01
2	541	0	0.524	Granite	12.75	3.0-6.5	NH-IM-20-2(145)01
3	595	0	0.43	Granite	11.40	3.0-6.5	EDS00-0072-00(039)
4	600	0	0.47	Granite	11.62	3.0-6.5	NHS00-0005-00(320)
5	580	12.20	0.493	Granite	12.54	3.0-6.5	NH-IM-20-2(145)01
6	579	19.69	0.446	Granite	11.67	3.0-6.5	CSNHS-M002-00(965)01
7	622	26.00	0.422	Granite	12.14	3.0-6.5	NHS-M002-00(434)01
8	605	20.66	0.43	Dolomite	12.09	3.0-6.5	NHSTP-0075-03(203)
9	590	18.64	0.438	Granite	10.87	3.0-6.5	CSSTP-0007-00(239)01
10	590	18.64	0.439	Dolomite	10.87	3.0-6.5	CSSTP-0007-00(239)01
11	600	20.16	0.47	Granite	11.42	3.0	IMNH0-0075-01(227)
12	600	20.16	0.47	Granite	11.42	6.5	IMNH0-0075-01(227)

By reviewing and analyzing these previous GDOT concrete mixtures, the project then created mixture IDs that would allow the team and fellow researchers to identify certain mixtures along with their material inputs easily. The project mixture IDs follow the order of characteristics of Table 23; for example, mixture number one's ID is (541/0FA/0.431/11.91G/4.9). By looking at this identification number, the researcher is aware that the mixture has 541 for its cementitious content, with the next number portraying the fly ash percentage; therefore, no fly ash is present in this mixture. The third number, 0.431, represents the water-to-cementitious ratio. The fourth part of the identification, 11.91G, represents two points of importance regarding the mixture's coarse aggregate. The number part of the 11.91G represents the coarse aggregate fraction, while the letter identifies which aggregate was used (G represents granite and D represents dolomite). The final number of the identification, 4.9, represents the mixture's air content that was determined in the fresh concrete property measurement. After adopting this naming method, Table 24 displays all twelve previously used GDOT mixtures.

Table 24. Concrete Mixture Identification

Mixture Number	Mixture ID	Cementitious Content (lbs/yd^3)	Fly Ash (%)	w/cm	CA Type	CA Fraction	Air Content (%)
1	541/0FA/0.431/11.91G/4.9	541	0	0.431	Granite	11.91	3.0-6.5
2	541/0FA/0.524/12.75G/4.0	541	0	0.524	Granite	12.75	3.0-6.5
3	595/0FA/0.43/11.4G/6.2	595	0	0.43	Granite	11.4	3.0-6.5
4	600/0FA/0.47/11.62G/6.1	600	0	0.47	Granite	11.62	3.0-6.5
5	580/12.2FA/0.493/12.54G/4.5	580	12.2	0.493	Granite	12.54	3.0-6.5
6	579/19.69FA/0.446/11.67G/5.5	579	19.69	0.446	Granite	11.67	3.0-6.5
7	622/26FA/0.422/12.14G/3.1	622	26	0.422	Granite	12.14	3.0-6.5
8	605/20.66FA/0.43/12.09D/5.0	605	20.66	0.43	Dolomite	12.09	3.0-6.5
9	590/18.64FA/0.438/10.87G/4.9	590	18.64	0.438	Granite	10.87	3.0-6.5
10	590/18.64FA/0.439/10.87D/5.9	590	18.64	0.439	Dolomite	10.87	3.0-6.5
11	600/20.16FA/0.47/11.42G/3.6	600	20.16	0.47	Granite	11.42	3
12	600/20.16FA/0.47/11.42G/4.7	600	20.16	0.47	Granite	11.42	6.5

KEY: 541/0FA/0.431/11.91G/4.9

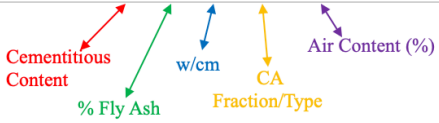

7.2 Test Results

7.2.1 Fresh Concrete Properties Results

Figures 9, 10, and 11 contain the concrete fresh property test results of the three different trials used in this study. Trial 1 refers to the properties measured in the previous study completed by Wing (2018); CTE specimens were batched during this trial. The second trial of concrete mixtures was used for the ultimate shrinkage and MOR testing. The third trial of concrete mixtures was batched for thermal conductivity testing. The three trials are plotted to demonstrate homogeneity across the various concrete mixing trials used in this study.

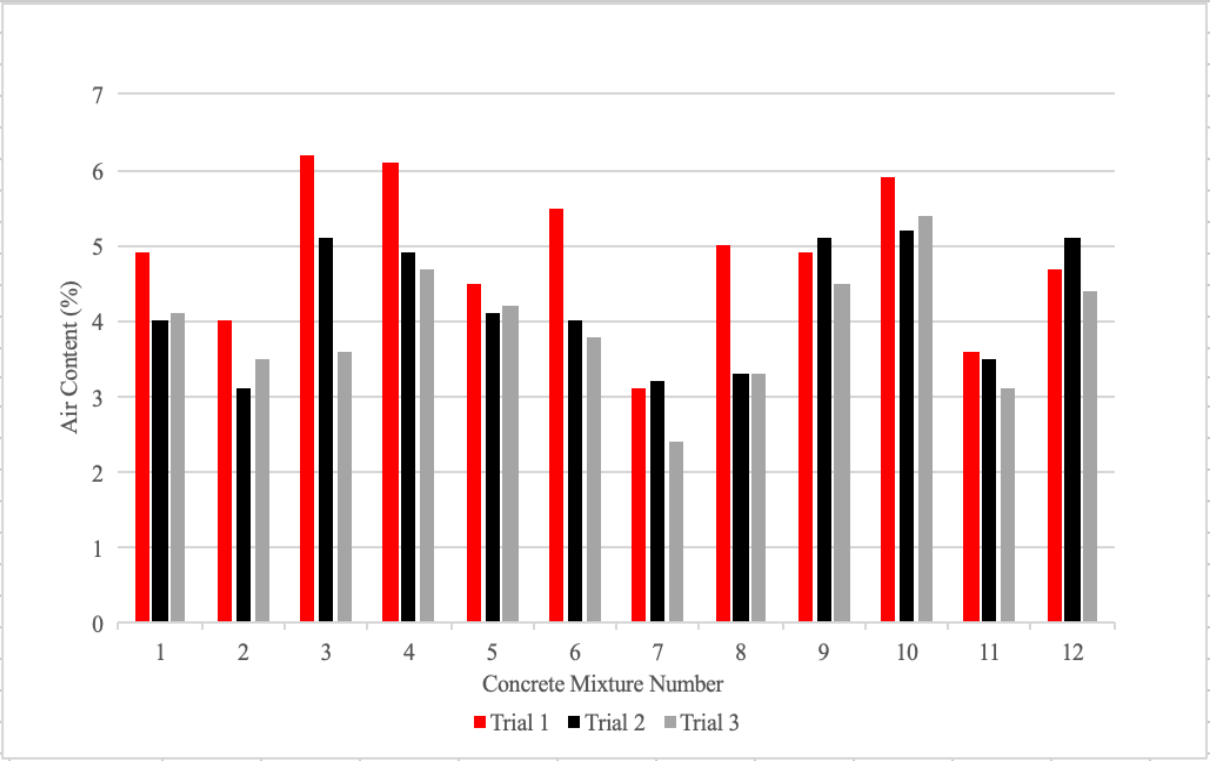

Figure 9. Air Content Comparison for Different Mixture Trials

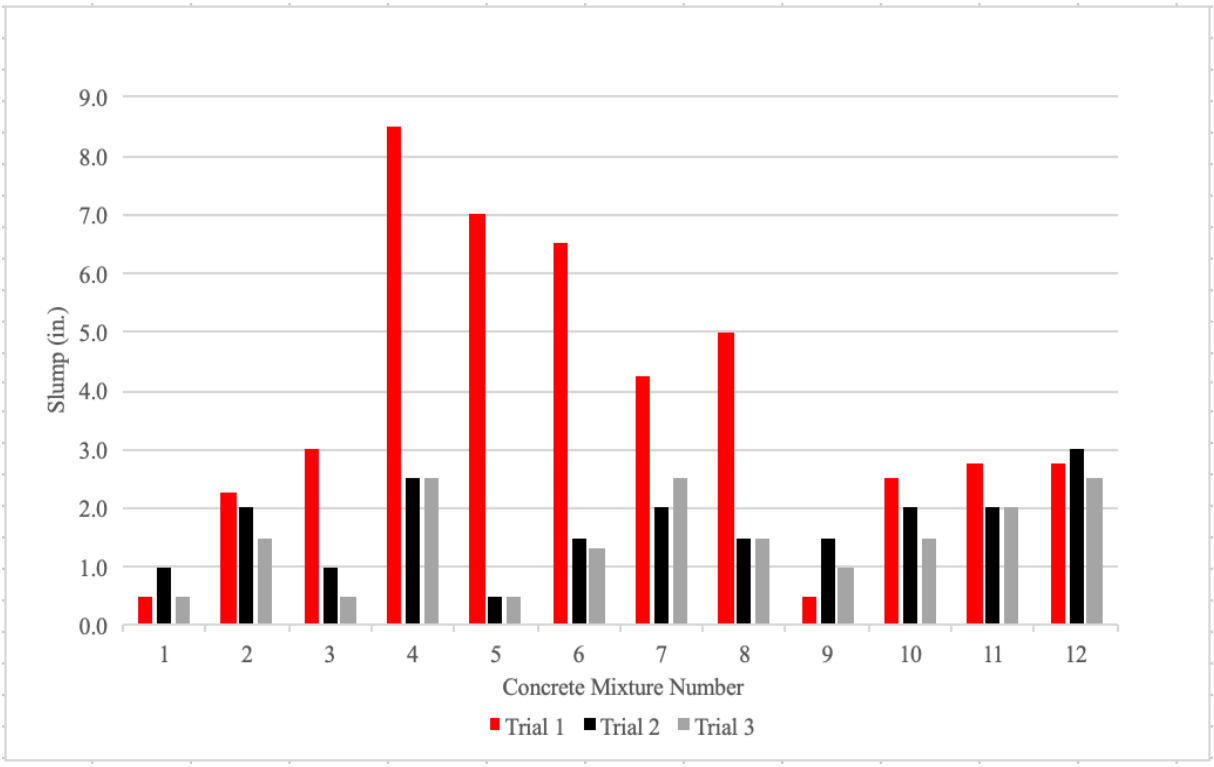

Figure 10. Slump Comparison for Different Mixture Trials

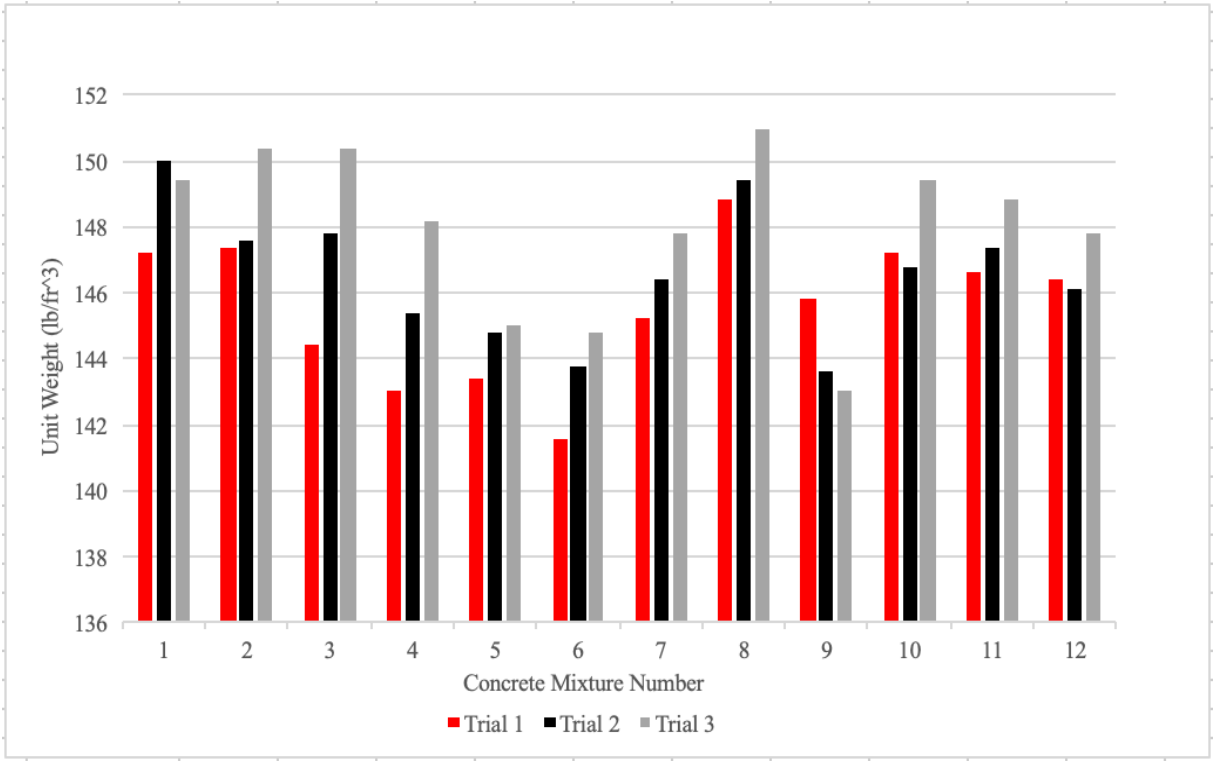

Figure 11. Unit Weight Comparison for Different Mixture Trials

The three different trials displayed fairly similar fresh concrete property results that provided quality assurance for the research team. Figure 9 proved that most of the concrete air content measurements were in the desired range of 3.0 to 6.0%. The concrete mixtures were desired to maintain slump values below 3.50 inches (88.9 mm). None of the mixtures in the second and third trials exceeded this maximum value. In some cases, trial 1 demonstrated a slight variation from the other two trials. During this initial batching process, fresh air content measurements were lower than expected. Higher dosages of air-entraining admixture (AEA) were used to combat this issue. This increased admixture usage related directly to the increased slump and air content measurements displayed in Figures 9 and 10. The research team then discovered that these distorted air content measurements were due to a malfunction in the air meter. A new air meter was purchased, and the mixture's AEA dosage returned to normal and provided the desired fresh property measurements in the second and third trials. The results illustrated in Figure 11 provided the expected results. A typical unit weight range includes 143.0 to 149.0 pcf (2290.6 to 2386.8 kg/m^3) for concrete mixtures. Some of the unit weight tests exceeded this 149.0 pcf (2386.8 kg/m^3); however, the difference was negligible, and the typical value used in GDOT pavement ME design is 150.0 pcf (2402.8 kg/m^3).

7.2.2 Mechanical Properties Test Results

Two trials of MOR testing are presented in Table 29 and Figure 12. Trial 1 was conducted by Wing (2018), where three 3 x 4 x 16" (76.2 x 101.6 x 406.4 mm) small beams and three 6 x 6 x 22" (152.4 x 152.4 x 558.8 mm) large beams were tested for MOR values and then compared using a linear regression model for validating the results. In trial 2, the twelve GDOT approved mixtures were batched again and, two 6 x 6 x 22" (152.4 x 152.4 x 558.8 mm) large beams were tested to validate the previous study results. Each mixture had two large beams to compare to the

previous data at 28 and 90-day testing periods. The 28-day and 90-day test results are listed in Table 25.

Table 25. MOR Test Results

Mixture Number	28-Day MOR (psi)		90-Day MOR (psi)	
	Trial 1	Trial 2	Trial 1	Trial 2
1	710	820	730	675
2	725	650	730	701
3	805	795	690	790
4	665	740	665	740
5	650	630	720	725
6	620	640	730	750
7	670	650	720	875
8	660	770	765	980
9	700	670	755	825
10	635	790	765	925
11	785	660	755	805
12	715	705	740	765

Results between the two trials demonstrated similar trends. However, it is important to note that the recent MOR test values only contain one large beam specimen's test value. Any variance between the results is likely due to the single large beam specimen test value serving as an outlier. The two trials' MOR test results are compared in Figure 12.

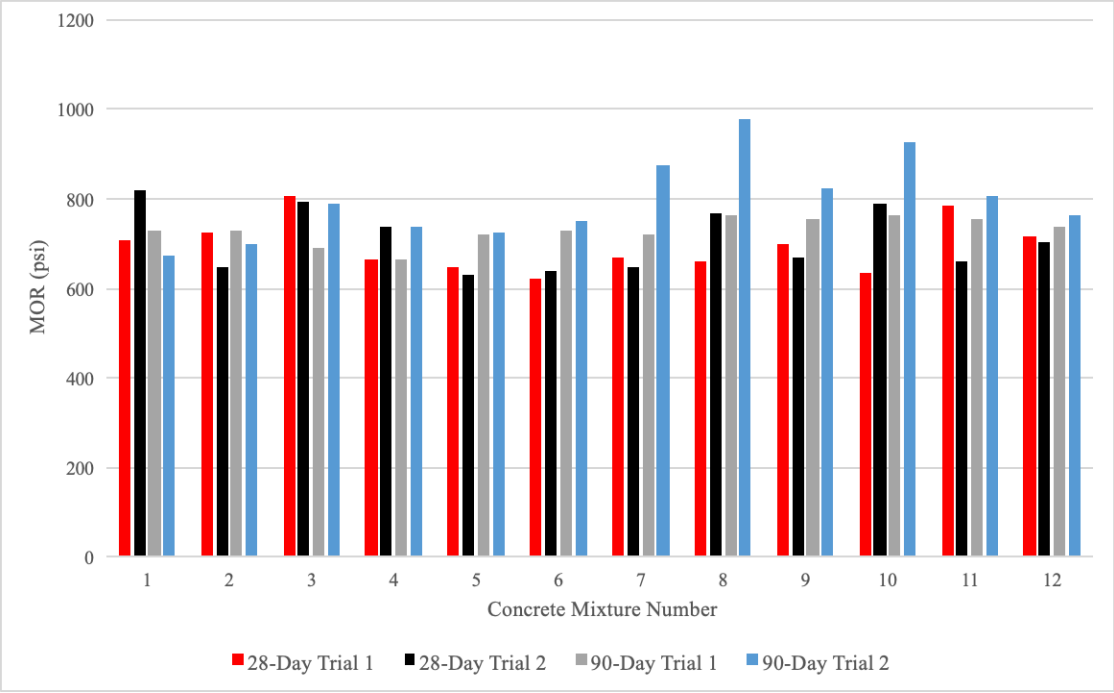

Figure 12. MOR Test Results Comparison

Figure 12 showed a similar trend between the mixtures. This validated the previous MOR results and reassured GDOT engineers when using MOR test values in the concrete mechanical properties database created by Wing (2018).

Ultimate shrinkage is either calculated or user-defined in level 2 and 3 designs in the Pavement ME software, and a user-defined input for a level 1 design is required. Due to ultimate shrinkages specimen's sensitivity, the specimens were stored in an environmental chamber that maintained a temperature of 73± 3 °F (23± 2°C) and relative humidity of 50 ± 4%. The shrinkage specimens were wet cured for the first 28-day period in this controlled environment and then removed from the curing tanks, where they continued to age in the controlled conditions provided by the environmental chamber. The ultimate shrinkage test results are listed in Table 26.

Table 26. Ultimate Shrinkage Test Results

Mixture Number	Age of Specimens (days)										
	3	7	14	28	35	42	49	56	63	70	77
	Average Percent Difference in Specimen Length (%)										
1	0.0003%	0.0007%	0.0040%	0.0013%	0.0023%	0.0030%	-0.0010%	-0.0037%	-0.0073%		
2	0.0010%	0.0000%	-0.0007%	-0.0007%	-0.0010%	-0.0007%	-0.0053%	-0.0083%	-0.0113%		
3	0.0030%	0.0057%	0.0060%	0.0013%	-0.0023%	-0.0043%	-0.0067%	-0.0090%			
4	0.0057%	0.0077%	0.0107%	0.0077%	-0.0007%	-0.0020%	-0.0120%	-0.0187%			
5	-0.0057%	-0.0007%	0.0020%	-0.0017%	-0.0037%	0.0013%	-0.0023%	-0.0007%	-0.0027%	-0.0107%	-0.0167%
6	-0.0057%	0.0010%	0.0030%	0.0007%	-0.0003%	-0.0020%	-0.0040%	-0.0047%	-0.0070%	-0.0150%	-0.0207%
7	-0.0007%	0.0037%	0.0050%	0.0047%	0.0033%	0.0037%	0.0043%	0.0027%	0.0027%	-0.0063%	-0.0120%
8	0.0093%	0.0140%	0.0160%	0.0077%	0.0057%	0.0043%	0.0030%	-0.0053%			
9	0.0083%	0.0103%	0.0107%	0.0080%	0.0097%	0.0147%	0.0137%	0.0133%	0.0077%	-0.0067%	
10	0.0040%	0.0030%	0.0040%	-0.0010%	-0.0010%	-0.0010%	-0.0015%	-0.0050%	0.0133%		
11	0.0040%	0.0080%	0.0100%	0.0097%	0.0073%	0.0107%	0.0083%	0.0020%	0.0118%		
12	0.0014%	0.0041%	0.0038%	0.0028%	0.0040%	0.0056%	0.0042%	0.0024%	0.0026%		

The results contained the average of three shrinkage specimens tested following ASTM C157. The test results successfully passed the precision and bias criteria of water stored shrinkage requirements. None of the specimens exceeded a maximum range of 0.0266%, while the means between the same mixtures' specimens did not exceed 0.0074% in 95% of the results. A visualization of the shrinkage results up to the 77-day mark is provided in Figure 13.

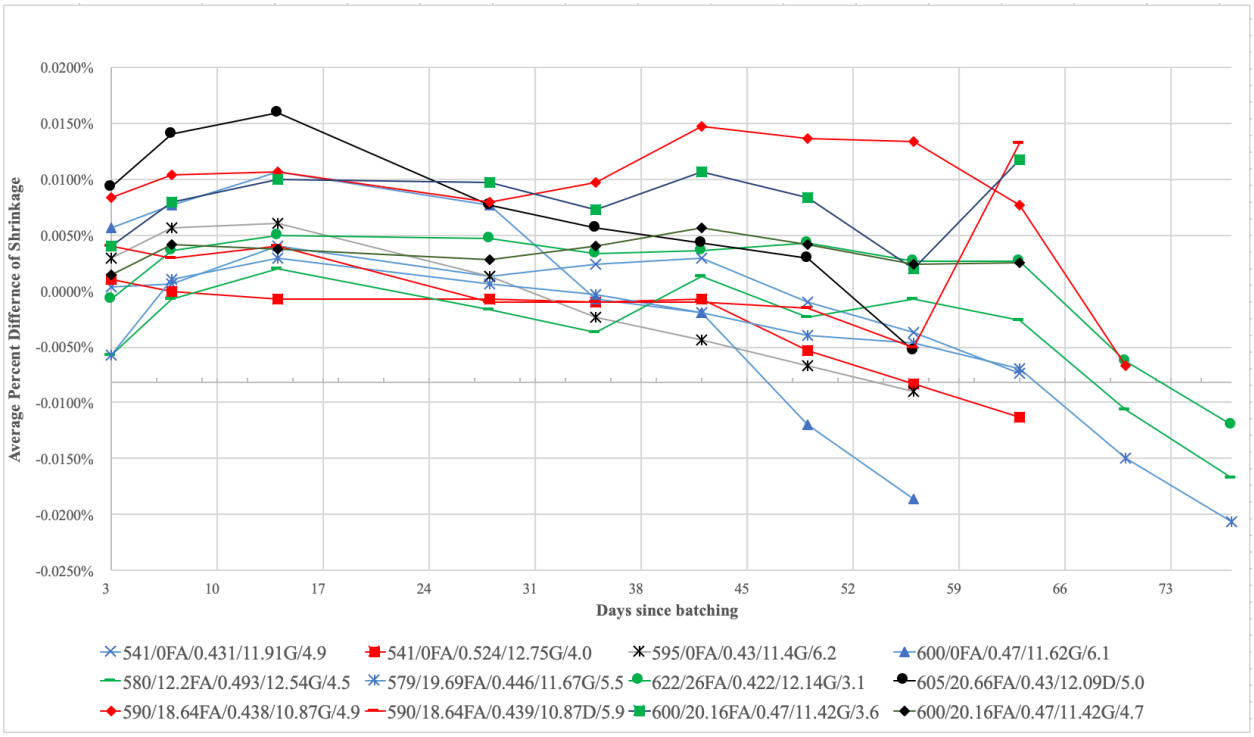

Figure 13. Ultimate Shrinkage Plot

A majority of the shrinkage specimens demonstrated an expected initial expansion during the first 14 days of the moisture-curing process. At the 28-day mark, specimens illustrated a shrinking trend. Mixtures containing fly ash had not fully cured at the 28-day mark and have slightly different shrinkage rates than the mixtures without fly ash. Conclusions regarding the ultimate shrinkage results will continue to be developed as later measurements are made.

7.2.3 Thermal Properties Test Results

The thermal properties test results are the primary focus of this study. The twelve GDOT approves mixtures were batched multiple times to achieve accurate lab-tested values that can be used for a MEPDG approach. The thermal properties of concern in this section are the coefficient of thermal expansion (CTE) and thermal conductivity. These properties were tested following the procedures mentioned in section 6.3.4. CTE test results are listed in Table 27.

Table 27. CTE Test Results

Mixture Number	Mixture ID	CTE (in/in/Fdeg)		
		Specimen 1	Specimen 2	Average
1	541/0FA/0.431/11.91G/4.9	4.81E-06	5.01E-06	4.91E-06
2	541/0FA/0.524/12.75G/4.0	4.62E-06	4.69E-06	4.66E-06
3	595/0FA/0.43/11.4G/6.2	5.18E-06	5.32E-06	5.25E-06
4	600/0FA/0.47/11.62G/6.1	5.03E-06	5.14E-06	5.09E-06
5	580/12.2FA/0.493/12.54G/4.5	5.07E-06	5.19E-06	5.13E-06
6	579/19.69FA/0.446/11.67G/5.5	5.22E-06	5.11E-06	5.16E-06
7	622/26FA/0.422/12.14G/3.1	5.39E-06	5.23E-06	5.31E-06
8	605/20.66FA/0.43/12.09D/5.0	5.33E-06	5.37E-06	5.35E-06
9	590/18.64FA/0.438/10.87G/4.9	5.39E-06	5.23E-06	5.31E-06
10	590/18.64FA/0.439/10.87D/5.9	5.43E-06	5.46E-06	5.45E-06
11	600/20.16FA/0.47/11.42G/3.6	5.02E-06	4.92E-06	4.97E-06
12	600/20.16FA/0.47/11.42G/4.7	4.99E-06	4.99E-06	4.99E-06

These results demonstrated expected trends between the concrete mixtures and typical characteristics of the thermal property. Previous research (Kim et al. 2012) concluded that the main factors affecting CTE were based on aggregates, mainly because of the amount of volume the mixture composed of the aggregate. Concrete mixtures containing dolomite, in particular, were proven to exhibit a higher CTE value than mixtures containing granite. Aggregate type displayed an obvious role in the test results shown in Table 27. The two mixtures, 8 (605/20.66FA/0.43/12.09D/5.0) and 10 (590/18.64FA/0.439/10.87D/5.9) that contained dolomite resulted in the two highest CTE values emphasizing the impact of the aggregate type on a concrete mixture's thermal properties.

CTE immediately provided accurate test results because the concrete cylinders for this property are tested in water in a saturated condition. During the initial thermal conductivity testing, variation in the test results that occurred due to the test specimens' varying moisture levels. As mentioned in section 6.3.4, the twelve mixtures were batched again and tested in three different moisture conditions. The thermal conductivity test results are located in Table 28.

Table 28. Thermal Conductivity Test Results

Mixture Number	Thermal Conductivity (BTU/ hr ft F)								
	Normal Condition			Oven Dry Condition			Saturated Condition		
	Specimen 1	Specimen 2	Average	Specimen 1	Specimen 2	Average	Specimen 1	Specimen 2	Average
1	1.054	1.104	1.079	0.789	0.936	0.863	1.428	1.426	1.427
2	1.191	1.269	1.230	0.507	0.573	0.540	1.634	1.559	1.597
3	1.143	1.152	1.148	0.606	0.540	0.537	1.539	1.522	1.531
4	1.213	1.190	1.202	0.463	0.464	0.464	1.507	1.427	1.467
5	1.160	1.164	1.162	0.469	0.806	0.638	1.688	1.609	1.649
6	1.059	1.023	1.041	0.934	0.887	0.911	1.686	1.690	1.688
7	1.354	1.628	1.491	1.048	0.915	0.982	1.535	1.904	1.720
8	1.481	1.929	1.705	1.615	1.640	1.628	2.225	2.273	2.249
9	1.734	1.745	1.740	0.922	0.934	0.928	1.890	1.783	1.837
10	1.407	1.557	1.482	1.399	1.195	1.297	2.104	2.082	2.093
11	1.160	1.282	1.221	0.972	0.900	0.936	1.517	1.693	1.605
12	1.054	1.217	1.136	0.720	0.488	0.604	1.346	1.362	1.354

These results demonstrate an expected trend between moisture and thermal conductivity. The two have a direct relationship with each other; as the moisture increases, so does the thermal conductivity test value. The oven-dry specimens provided the lowest test results because of the complete lack of moisture in the concrete cylinder undergoing the test. Similarly, the saturated specimens had the highest thermal conductivity results due to the specimen's high moisture content during testing. To provide the most uniform test results for the normal condition specimens, after they were removed from the curing tank, where they were stored for 28-days, they were placed in the environmental chamber for 24 hours. Density has proven to be another key factor affecting thermal conductivity. An extra cylinder was made for each concrete mixture to test for the density after the 28-day curing period. Table 29 contains the lab tested density values for each mixture.

Table 29. Density Measurements

Mixture Number	Mixture ID	Density (kg/m^3)	Density (lb/ft^3)
1	541/0FA/0.431/11.91G/4.9	2313.5	144.4
2	541/0FA/0.524/12.75G/4.0	2276.6	142.1
3	595/0FA/0.43/11.4G/6.2	2231.4	139.3
4	600/0FA/0.47/11.62G/6.1	2252.3	140.6
5	580/12.2FA/0.493/12.54G/4.5	2228.7	139.1
6	579/19.69FA/0.446/11.67G/5.5	2205.9	137.7
7	622/26FA/0.422/12.14G/3.1	2239.7	139.8
8	605/20.66FA/0.43/12.09D/5.0	2361.4	147.4
9	590/18.64FA/0.438/10.87G/4.9	2240.9	139.9
10	590/18.64FA/0.439/10.87D/5.9	2263.9	141.3
11	600/20.16FA/0.47/11.42G/3.6	2311.6	144.3
12	600/20.16FA/0.47/11.42G/4.7	2212.5	138.1

The values from Table 29 are used in Figure 14 to illustrate the role that density has on thermal conductivity in concrete. Concrete mixtures are expected to demonstrate an increase in thermal conductivity test results as the mixture's density increases.

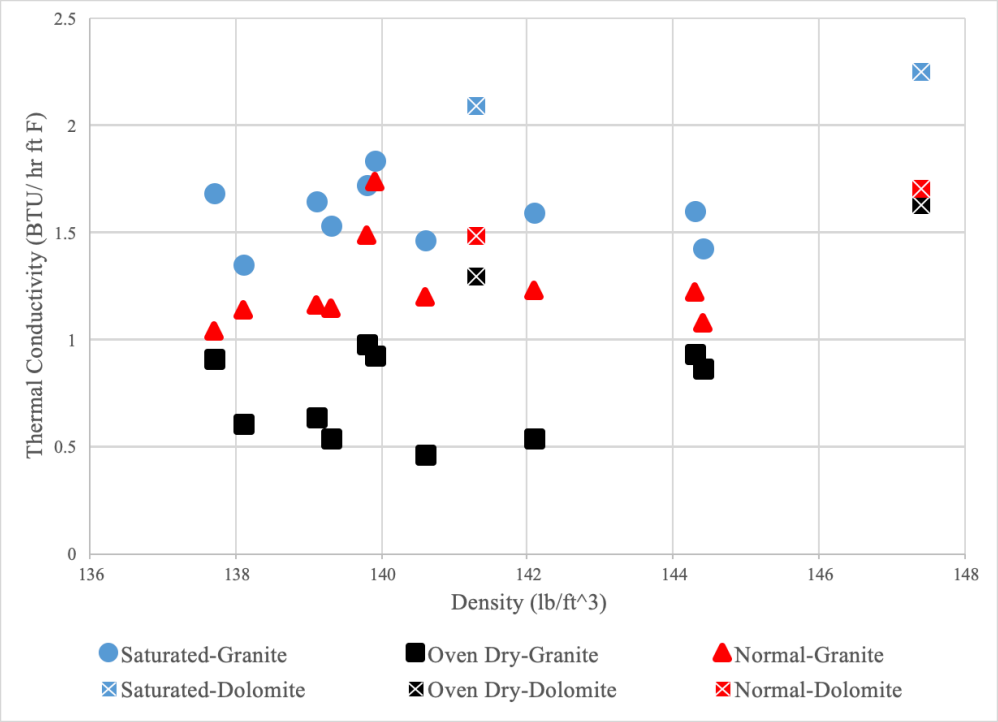

Figure 14. Effect of Density on Thermal Conductivity

Density exemplified an obvious effect on the thermal conductivity test results. Density has been proven to have a direct impact on thermal conductivity. Figure 14 supported this expected trend by displaying that a higher density generally resulted in a higher thermal conductivity test value. It is important to note that dolomite continues to show an effect on the thermal property test results. Concrete mixtures containing the dolomite aggregate reflected a higher thermal conductivity similar to its higher CTE values. Since a higher thermal conductivity value correlates with a better insulating material, it is important to highlight that dolomite's impact on thermal conductivity could minimize the negative impact of providing a higher coefficient of thermal expansion value. To understand this relationship between thermal conductivity, the two thermal properties are plotted together in Figure 15.

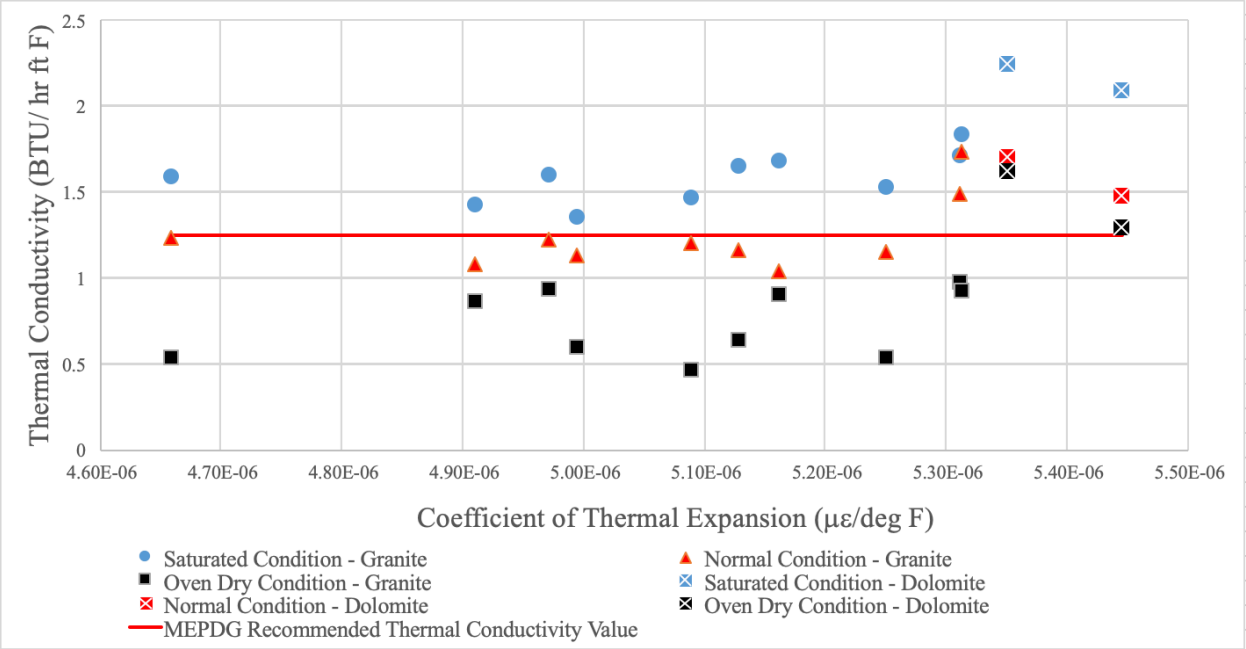

Figure 15. CTE and Thermal Conductivity Plot

A direct relationship between the two critical thermal properties was displayed. An increase in CTE increased thermal conductivity, with the two dolomite mixtures on the figure's far-right side portraying the extreme thermal values. Since thermal conductivity is not yet a commonly

performed test, GDOT employees could refer to this plot when looking for the best estimate option for a thermal conductivity test value-based on CTE when using the MEPDG approach.

7.3 Sensitivity Analyses Using Pavement ME

Initial analysis was performed on a JPCP structure at a level 3 input to determine how impactful the three thermal properties were to a rigid pavement structure. The sensitivity analyses were performed on the structure displayed in Figure 16. All of the inputs used in this sensitivity analysis followed the recommended input values for a JPCP structure by *The GDOT Pavement ME Design User Input Guide* (ARA, 2015), excluding the thermal property being analyzed. The structure contained five separate layers that would most represent a typical GDOT design. The top layer was a 10” PCC layer using the recommended concrete property values. The second layer contained a 3” asphalt concrete (AC) interlayer using SuperPave: 64-22. Underneath the interlayer, a 10” crushed gravel layer acted as the non-stabilized base. The structure then contained two subgrade A-7-6 sections at the bottom. A 12” compacted subgrade layer on the top was used to replicate typical GDOT practice, and the bottom subgrade portion acted as a semi-infinite layer.

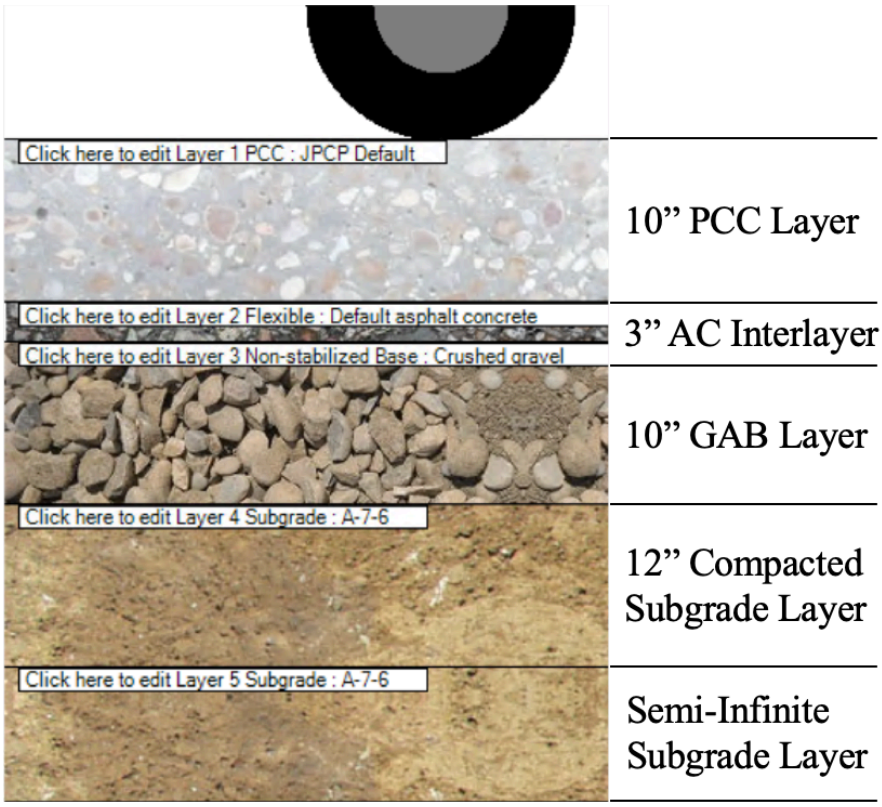

Figure 16. JPCP Structure used in Sensitivity Analysis

Sensitivity Analyses were performed using a level 3 design for a JPCP structure. These initial investigations were used in determining the relevance of the thermal properties, and the role they play in predicting the pavement distresses in Pavement ME software.

7.3.1 Sensitivity Analyses for CTE

The initial analyses were performed for CTE on a JPCP structure. CTE has previously been proven to be the most impactful thermal property input. During these analyses, the base values of heat capacity and thermal conductivity were used, 0.28 BTU/lb-deg F and 1.25 BTU/hr-ft-deg F, respectively. Two additional analyses were performed using the extreme lab-tested thermal conductivity values of 0.464 and 2.249 BTU/hr-ft-deg F as base values. The analyses used a 0.4 με/deg F increment for CTE values ranging from 4.70 to 8.0 με/deg F. The lower value was selected because it was close to the lowest lab-tested CTE value, and the higher value of 8.0 με/deg

F was selected to clearly demonstrate the trend between CTE and the performance indicator of concern.

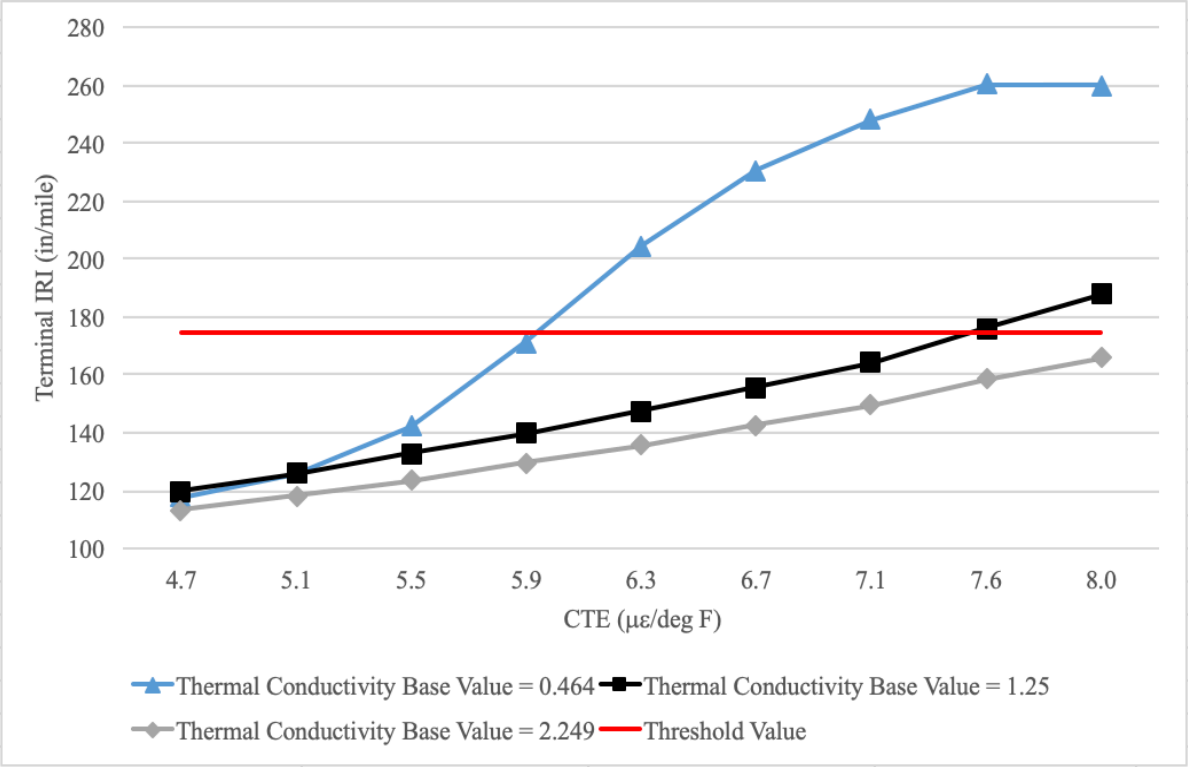

Figure 17. CTE's Effect on Terminal IRI

Figure 17 illustrated an expected relationship between CTE and terminal IRI. A higher CTE value is typically correlated to an IRI increase due to the higher cracking and faulting. The analyses containing the extreme lab-tested thermal conductivity values showed a dramatic effect on pavement performance prediction. A higher thermal conductivity value is expected to provide less pavement distress due to its ability to insulate the PCC layer better. The test containing the higher thermal conductivity base value of 2.249 BTU/hr-ft-deg F supported this expectation by resulting in a slightly lower terminal IRI prediction. The analysis containing the smaller thermal conductivity base value of 0.464 BTU/hr-ft-deg F differed from the other trials and demonstrated a rapid increase in terminal IRI prediction after the typical CTE value of 5.1 με/deg F was

surpassed. These analyses proved that CTE and thermal conductivity play a crucial role in predicting pavement distresses in the MEPDG approach.

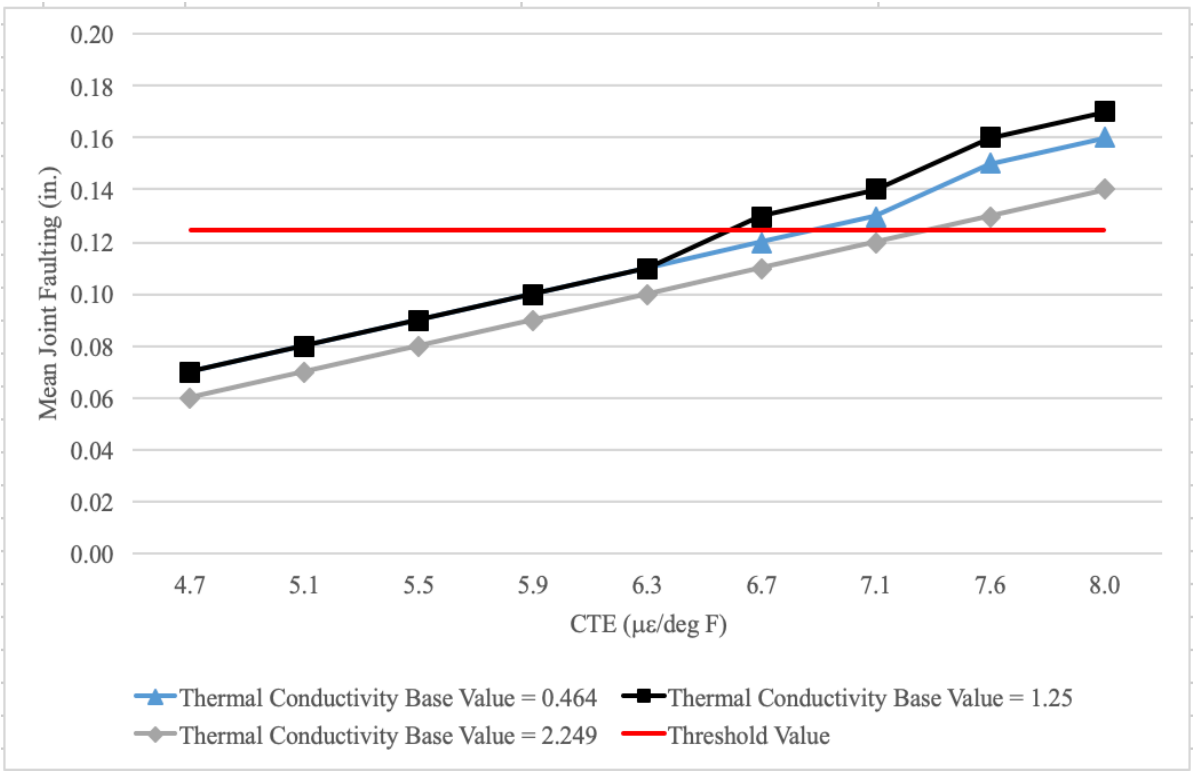

Figure 18. CTE's Effect on Mean Joint Faulting

Figure 18 provides important insight into the impact CTE plays in the faulting of a pavement structure. A study performed by Mallela et al. (2005) highlighted the impact that CTE has on mean joint faulting. These analyses supported that higher CTE values are expected to result in an increased mean joint faulting. Once again, the analysis using the high thermal conductivity base value displayed less predicted distress.

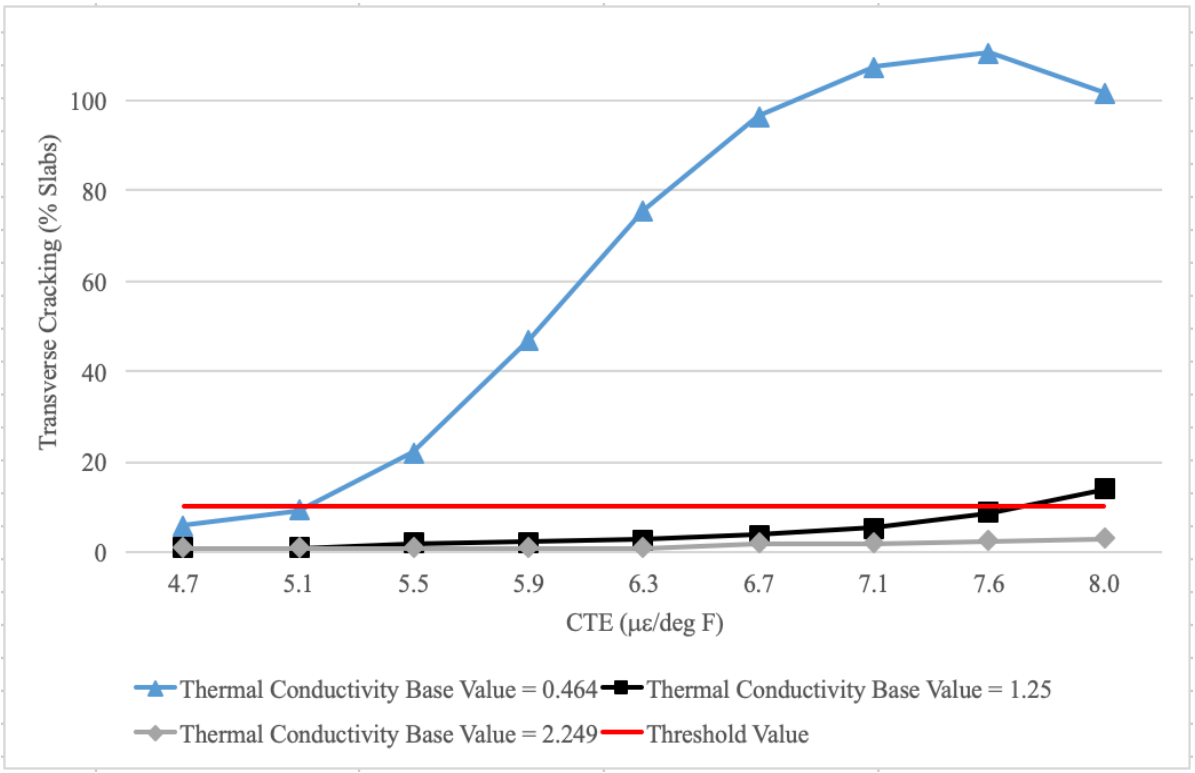

Figure 19. CTE's Effect on Transverse Cracking

Figure 19 proved that higher CTE values affected the transverse cracking of the pavement structure. Field studies have proven higher CTE values allow for an increase in transverse cracking primarily because of the PCC mixture's curling behavior. This curling occurs primarily due to temperature variation throughout the concrete layer, which increases along with an increase in CTE. It is important to note the behavior of the analysis using a low thermal conductivity base value. This analysis exhibited a dramatic increase in cracking prediction compared to the other analyses using higher thermal conductivity values. Figure 19 proved that both thermal conductivity and CTE played a critical role in transverse cracking prediction in MEPDG.

7.3.2 Sensitivity Analyses for Thermal Conductivity

The sensitivity analyses conducted for thermal conductivity ranged from 0.44 to 2.30 BTU/hr-ft-deg F. These values were selected based on lab-tested values for the twelve GDOT

approved mixtures. For these analyses, the default values of 5.1 x 10^{-6} με/deg F and 0.28 BTU/lb-deg F were used for CTE and heat capacity, respectively. Two additional analyses were performed for each pavement distress using the extreme lab-tested CTE values of 4.66 and 5.45 με/deg F as base values.

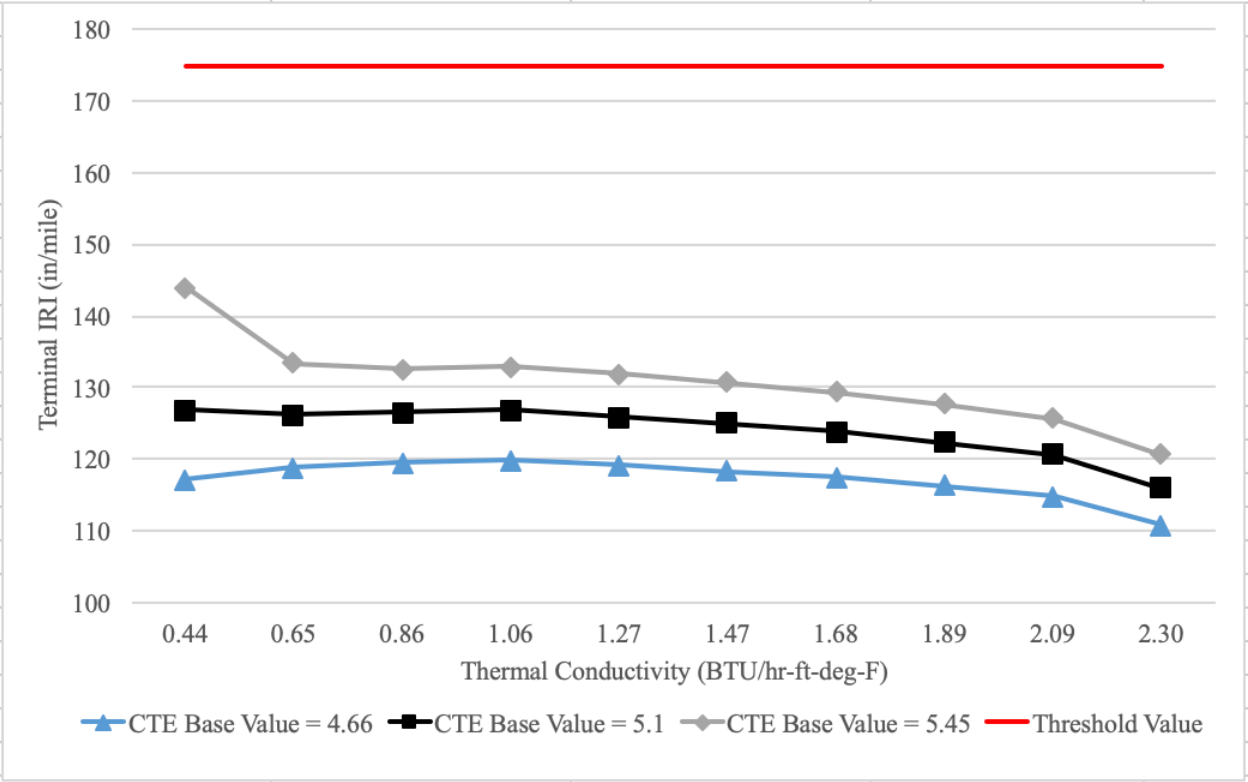

Figure 20. Thermal Conductivity's Effect on Terminal IRI

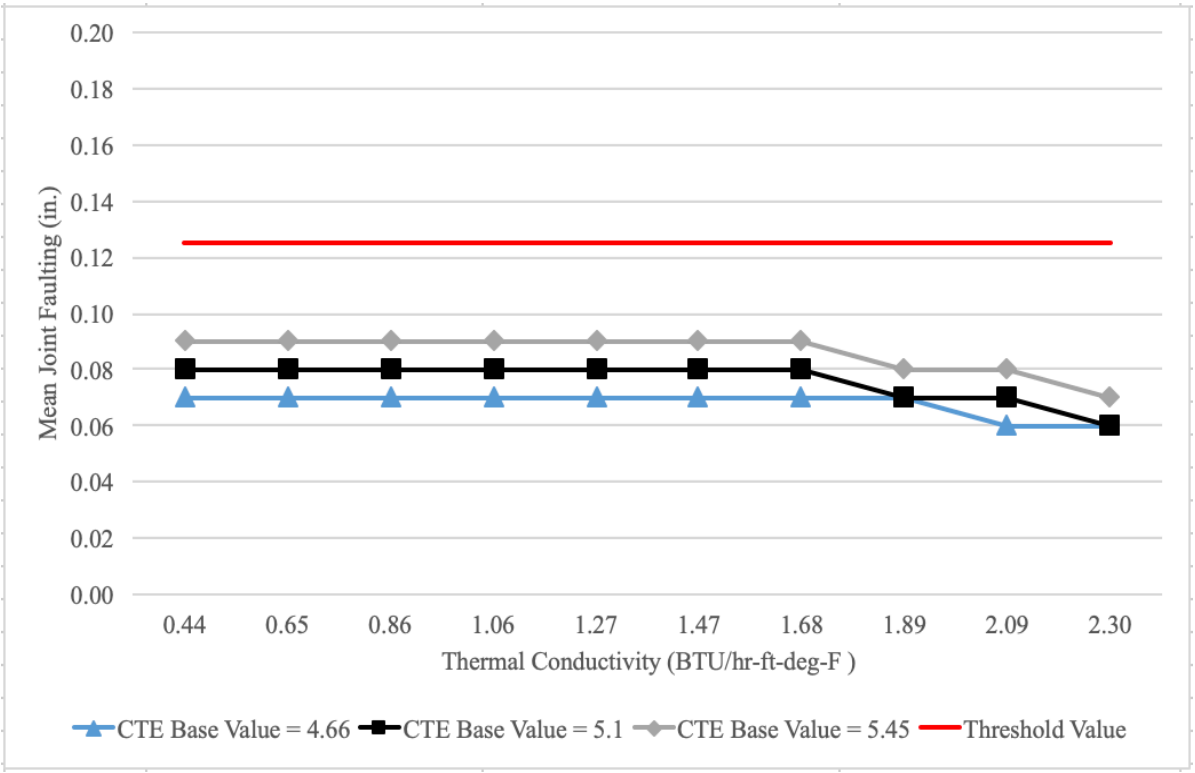

Figure 21. Thermal Conductivity's Effect on Mean Joint Faulting

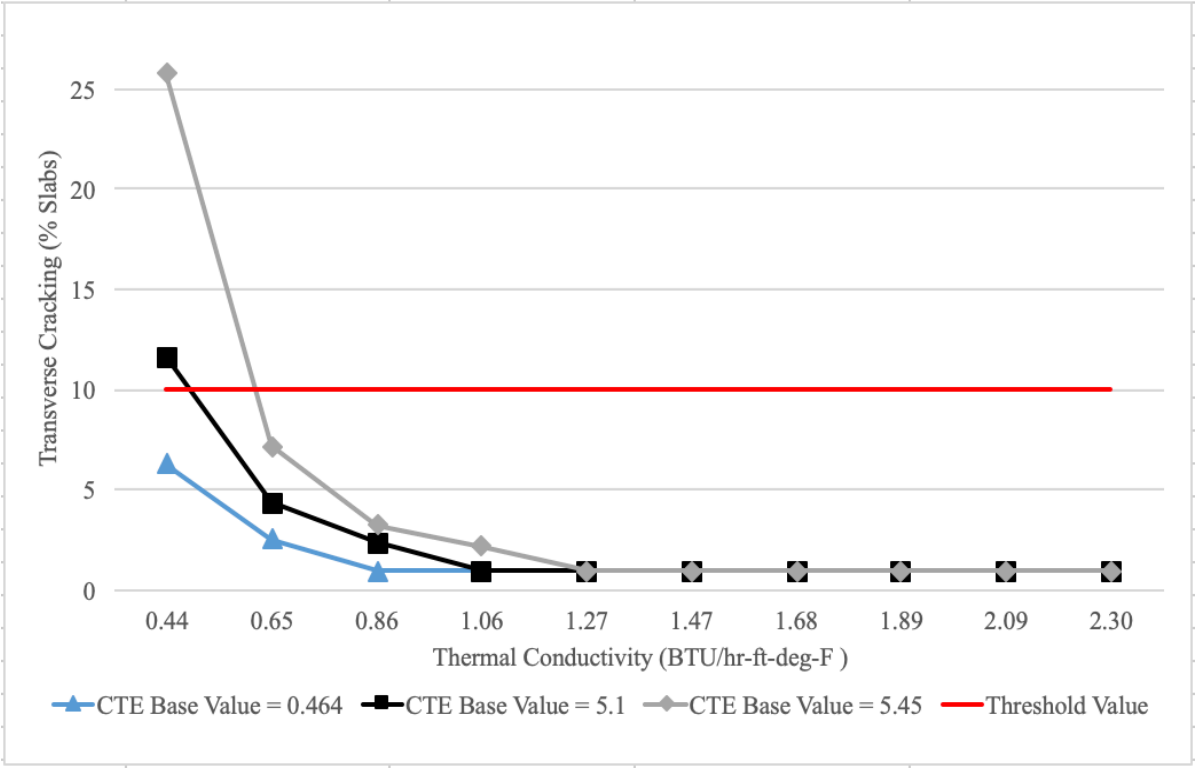

Figure 22. Thermal Conductivity's Effect on Transverse Cracking

Figures 20 and 21 demonstrated little interaction between the Pavement ME predicted distresses and change of thermal conductivity values. The lower thermal conductivity values resulted in higher predicted distresses; however, CTE exhibited a more impactful effect in the distress prediction process. Figure 22 illustrated that a lower thermal conductivity value created a higher predicted transverse cracking percentage. This explained the dramatic trend in Figure 19 and supported that a decrease in thermal conductivity reduces the concretes ability to insulate temperature changes and, in return, prevent the structure's ability to release heat flow efficiently. Due to this interaction between the heat and pavement, a lower thermal conductivity resulted in more distresses, specifically transverse cracking. While thermal conductivity in the PCC layer decreased, the thermal diffusivity also decreased the layer's effectiveness as a thermal buffer resulting in higher predicted distresses.

7.3.3 Sensitivity Analyses for Heat Capacity

Heat capacity was the final thermal property to undergo inspection with Pavement ME's predicted distresses. The heat capacity values ranged from 0.20 to 0.32 BTU/lb-deg F. These values were selected based on typical PCC heat capacity values, with the default value for heat capacity in the MEPDG being 0.28 BTU/lb-deg F and the 0.32 BTU/lb-deg F exceeded the recommended value for the software. For these analyses, the default values of 5.1 με/deg F and 1.25 BTU/hr-ft-deg-F were used for CTE and thermal conductivity, respectively. Extreme base values for CTE and thermal conductivity were investigated; however, the Pavement ME software would not allow these analyses to be run due to a "stability failure" in the program.

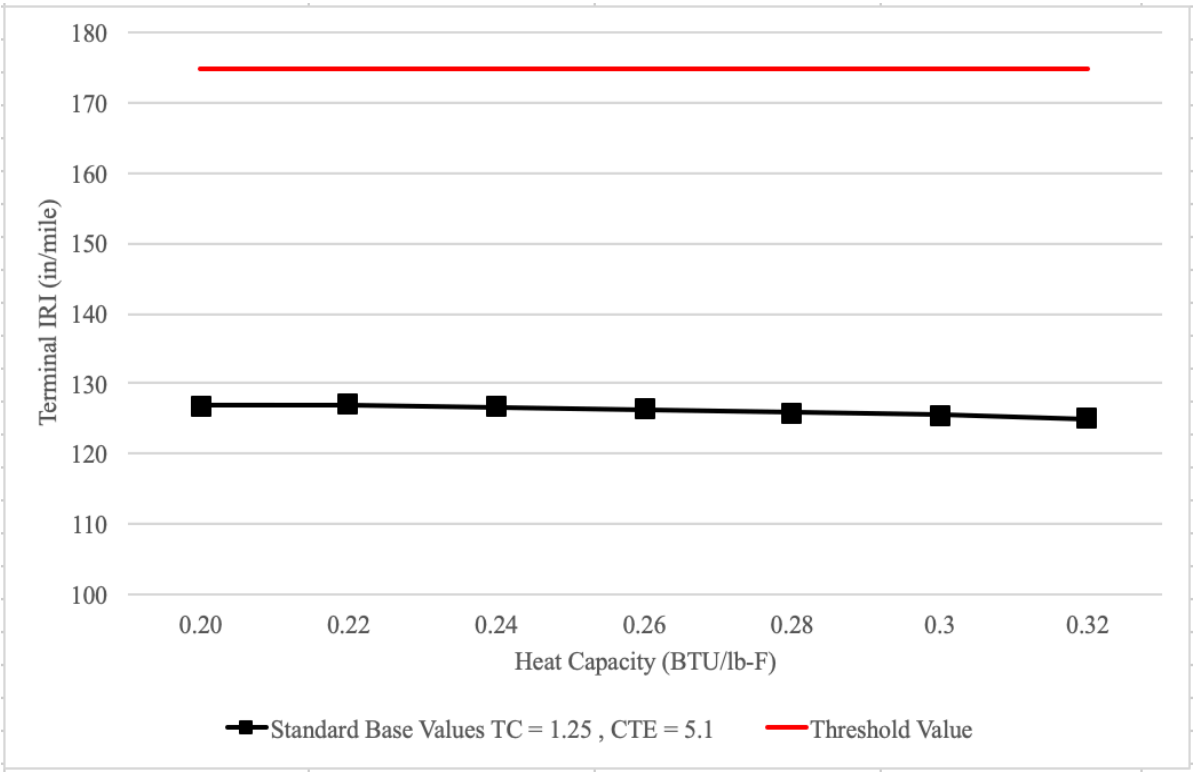

Figure 23. Heat Capacity's Effect on Terminal IRI

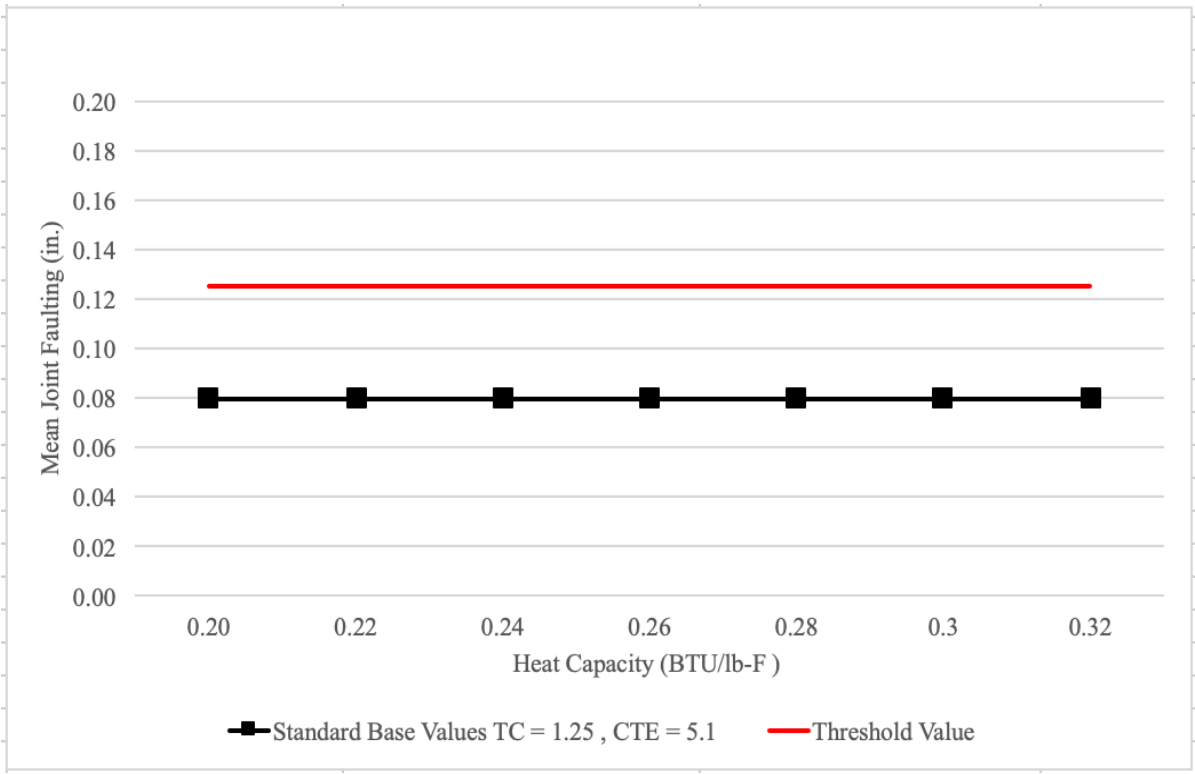

Figure 24. Heat Capacity's Effect on Mean Joint Faulting

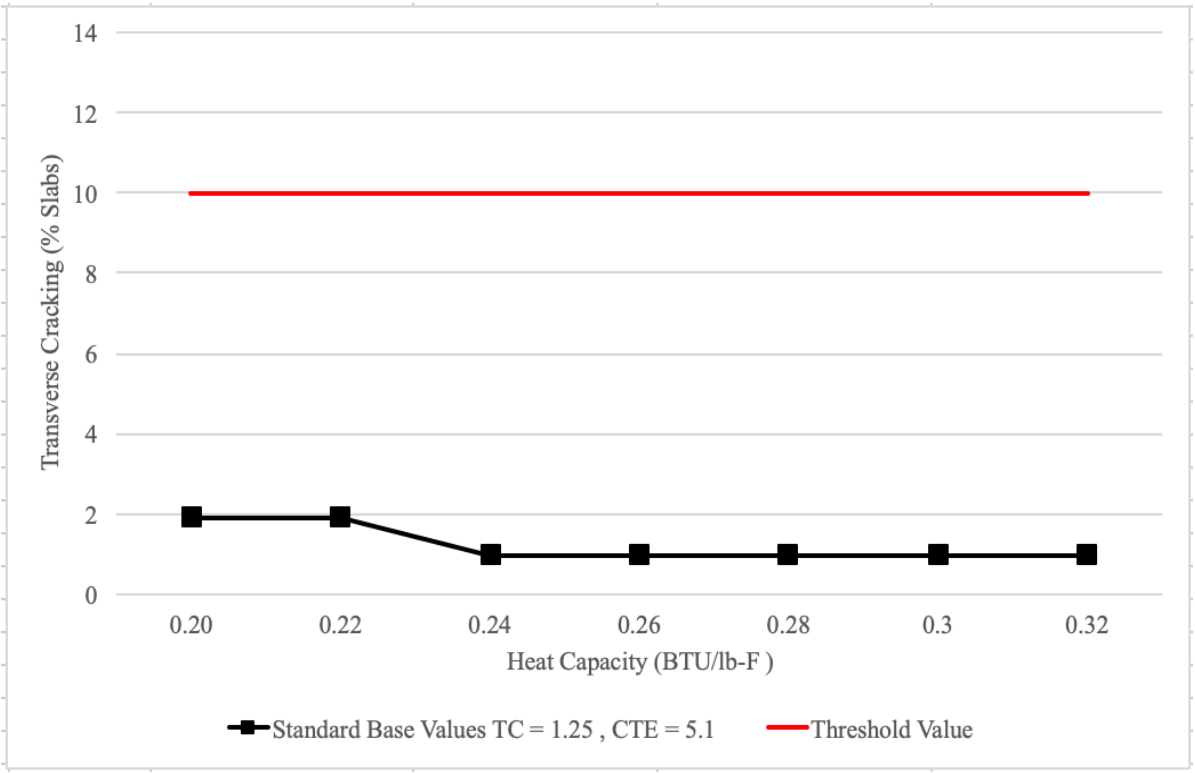

Figure 25. Heat Capacity's Effect on Transverse Cracking

Figures 23, 24, and 25 demonstrated little interaction between this heat capacity and the pavement performance predictions. Previous studies similarly determined this thermal property to have minimal impact on the distress predictions. Due to its limited role in the MEPDG prediction process, the recommended heat capacity value of 0.28 BTU/lb-deg F should continue to be used as the default input for this thermal property.

8.0 UNDERSTANDING THE RELEVANCE OF MIXTURE INPUTS USING MACHINE LEARNING TECHNIQUE

8.1 Machine Learning Introduction

The use of machine learning (ML) to estimate concrete properties based on the mixture design parameters helps understand the impact that various concrete mixture constituents may have on thermal concrete properties. ML was first introduced in the 1960s, and decision trees, being one of the most popular and accurate prediction models, have been vastly used in many different fields because they are easy to use, lack obscurity, and better deal with missing values (Y. song, 2015). Machine learning applications in engineering have increased in recent years, and the growth is expected to continue due to its benefits offered in improved prediction accuracy of composite materials (B. Boukhatem, 2011). However, due to the concrete's complexity as a composite material, the concrete's properties' predictability has been challenging.

Due to the large number of uncontrollable variables associated with a concrete mixture, the interactions and confounding effects among those variables are complex to model, which often results in lower prediction accuracy when a larger number of factors, both controlled and uncontrolled, are involved (D.C. Montgomery, 2017).

Machine learning is typically used for developing predictive models, either for classification or regression. Revealing the relationship between a dependent variable and one or more independent variables is the main focus of regression (M. Hofmann, 2013).

Previous studies have been conducted with machine learning applications for estimating concrete properties. Chopra and Sharma looked into the use of three models in the prediction of concrete compressive strength, including the random forest (RF) model, decision tree (DT) model, and neural network (NN) model. This study's results are illustrated in Table 30 and depict that the

NN model was the best primarily because of its ability to approximate the nonlinear relationship between input-output features (P. Chopra, 2018).

Table 30. Results of Training and Validation DT, RF, and NN Models (P. Chopra, 2018)

Model	Curing age	Results of training set		Results of validation set		Results of testing set	
		R^2	RMSE	R^2	RMSE	R^2	RMSE
DT	28 days	0.7167	3.0717	0.4534	3.7188	0.4388	3.9073
	56 days	0.8604	2.0111	0.7519	2.4596	0.8008	2.2514
	91 days	0.8785	1.8454	0.8835	1.7957	0.8270	1.8294
RF	28 days	0.9426	1.6433	0.7943	1.3400	0.6870	2.6912
	56 days	0.9670	1.1306	0.9343	1.7282	0.9058	1.1449
	91 days	0.9780	0.8957	0.9828	1.6123	0.9213	1.0700
NN	28 days	0.9599	0.7251	0.9476	0.8213	0.9460	0.8106
	56 days	0.9769	0.7176	0.9872	0.8099	0.9500	0.9100
	91 days	0.9770	0.8023	0.9824	0.9641	0.9562	0.9106

When exploring the best model for our data, Song and Lu demonstrated the advantages of the decision tree (DT) method. The DT method is a robust statistical tool for predicting and interpreting data that has several potential applications. This method simplifies complicated relationships between input and output variables by breaking down these input variables into notable subgroups. This method is easy to analyze and understand complex composite materials, such as concrete (Y. Song, 2015).

A principal component analysis was performed to understand the sensitivity of CTE outputs by Kim (2014). Eight inputs listed in Table 31 were examined in determining their individual impact on CTE. This principal component analysis was only a part of developing an accurate estimation of CTE input values for the Mechanistic-Empirical design of concrete pavements. Kim (2014) tested and compared two separate model forms, Artificial Neural Networks (ANN) and Response Surface Models (RSM), based on a 2^k experimental design. Both models proved reliable forms of estimation; however, the ANN generated more accurate results.

Table 31. ANN Architecture Inputs in CTE Estimation (Kim, 2014)

ANN Layer	Neuron		Value	
			Low	High
Input	Aggregate	Granite (kg/m^3)	682	1246
		Dolomite (kg/m^3)	682	1246
	Sand	Granite Gneiss Manufactured Sand (kg/m^3)	564	1128
		Alluvial/Marine natural sand (kg/m^3)	564	1128
	Fly Ash	C-Ash (kg/m^3)	12	95
		F-Ash (kg/m^3)	12	95
	Cement (kg/m^3)		273	314
	AC (%)		3	6
Hidden	12 Hidden Neurons		n/a	n/a
Output	Coefficient of Thermal Expansion (με/°C)		5.81	9.94

Kim (2014) displayed the relevance that each input plays in estimating a mixtures CTE value. Table 32 displays the principal components' coefficients in increasing cumulative variation percentage from the left to right direction.

Table 32. Principle Components of Input Data (Kim, 2014)

Input parameter	Principal Component Coefficients							
1 Granite	-0.71	0	0.5	0	0	0	0	0.5
2 Dolomite	0.71	0	0.05	0	0	0	0	0.5
3 Granite Gneiss manufacture sand	0	0.71	-0.5	0	0	0	0	0.5
4 Alluvial/Marine natural sand	0	-0.71	-0.5	0	0	0	0	0.5
5 C-Ash	0	0	0	0.71	-0.55	0.43	0	0
6 F-Ash	0	0	0	-0.7	-0.59	0.41	0	0
7 Cement	0	0	0	-0.02	0.59	0.81	-0.01	0
8 AC	0	0	0	0	0	0.01	1	0
Cumulative variation (%)	51.2	91.6	99.6	99.9	100	100	100	100

Gradient boosting machine (GBM) is a powerful ensemble-based machine learning algorithm adopted in this study. In a study conducted by Boehmke, the GBM demonstrated a continuous improvement in tree learning by combining weak and shallow successive trees. While combining various sequential weak trees, an accurate prediction model is formed (Boehmke, 2018). This improvement process highlighted that GBM would help determine the various mixture inputs relevant to the concrete thermal property. To develop of ensemble models, it is essential to

fine-tune several hyperparameters, often conducted using the cross-validation technique. For example, the key hyperparameters for GBM are shown in Table 33.

Table 33. Gradient Boosting Machine Hyperparameters

Hyperparameter	Ideology
Number of trees	The ideal number of trees to fit
Depth of trees (interaction.depth)	The depth of splits, which controls the complexity of GBM
Learning rate (shrinkage)	Determines the rate at which the algorithm learns at each round of boosting.
Subsampling	Determines if a percentage of the accessible training observations are utilized or not
Cross-validation (cv.fold)	5-fold cross-validation utilized in this study
Observations (n.minobsinnode)	The minimum number of observations permitted in each terminal node

8.2 Analysis and Results

As GDOT completes the transition to a mechanistic-empirical design approach, it would be beneficial to further understand the relationships between the individual characteristics of a concrete mixture and how they impact the mixture's mechanical and thermal properties. For initial analysis, the thermal properties of concern are the coefficient of thermal expansion (CTE) and thermal conductivity. All of the thermal property lab-tested data from this study will be utilized in making conclusions based on the twelve GDOT approved concrete mixtures, along with CTE data from the study conducted by Kim (2014). GBM was selected to model the relationships of the concrete constituents with the resulting properties. Table 34 and Table 35 illustrate the input parameters utilized in developing the gradient boosting machines for CTE and thermal conductivity, respectively.

Table 34. Coefficient of Thermal Expansion Model Input Parameters

Parameter ID	Parameter Description
Cement	Cementitious content of the concrete mixture measured in (lbs/yd^3)
C_ash	Class type C fly ash content (lbs/yd^3)
F_ash	Class type F fly ash content (lbs/yd^3)
w_c	Water-to-cementitious ratio of the mixture
Granite	Coarse aggregate type for the mixture (lbs/yd^3)
Dolomite	Coarse aggregate type for the mixture (lbs/yd^3)
MS	Manufactured sand content (lbs/yd^3)
NS	Natural sand content (lbs/yd^3)
Air	Fresh property air measurement
CTE (response variable)	Coefficient of Thermal Expansion (με/deg F)

Table 35. Thermal Conductivity Model Input Parameters

Parameter ID	Parameter Description
Cement	Cementitious content of the concrete mixture measured in (lbs/yd^3)
F_ash	Class type F fly ash content (lbs/yd^3)
w_c	Water-to-cementitious ratio of the mixture
Granite	Coarse aggregate type for the mixture (lbs/yd^3)
Dolomite	Coarse aggregate type for the mixture (lbs/yd^3)
NS	Natural sand content (lbs/yd^3)
Air	Fresh property air measurement
Density	Concrete mixture density measurement (lb/yd^3)
Cond_S	Saturated condition during testing
Cond_N	Normal condition during testing
Cond_OD	Oven dry condition during testing
TC (response variable)	Thermal Conductivity (BTU/ hr ft F)

Once the parameters were defined, model development began using tree-based methods. Multiple regression methods exist which estimate the output value based on various input values of the dataset. GBMs were selected due to the high prediction accuracy and the versatility offered in the hyperparameter tuning options. After manually changing the hyperparameters, a realistic range of values was established for each parameter. The hyperparameters were tuned using a grid

search that evaluated a range of hyperparameter values and combinations and calculated the best set of hyperparameters. The selected hyperparameter values are shown in Table 36.

Table 36. Hyperparameter Tuning

Hyperparameter	CTE Model	TC Model
Number of trees	412	486
Interaction.depth	7	7
Shrinkage	0.05	0.3
N.minobsinnode	1	5
Bag.fraction	1	0.5

After the GBM hyperparameters were tuned for each thermal property, the GBMs prediction accuracies were assessed using the test dataset. Figure 26 illustrates the two machine learning models and the R^2 value associated with each GBM.

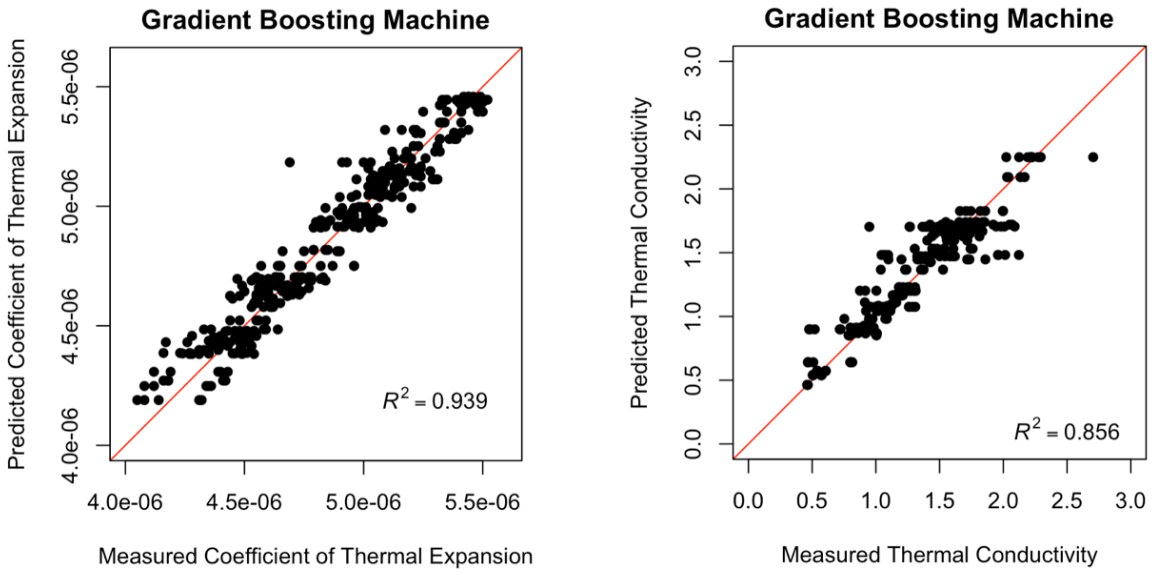

Figure 26. GBM Prediction Accuracies for Thermal Properties

The models provided R^2 values of 0.939 and 0.856 for CTE and thermal conductivity, respectively. The GBMs proved to be effective in predicting the thermal properties using the various concrete mixture inputs. The models were then used to determine how impactful each of

the concrete mixture design constituents was in estimating the thermal property of concern. The concrete mixture input's relative influence on the concrete mixture's thermal conductivity is displayed in Figure 27.

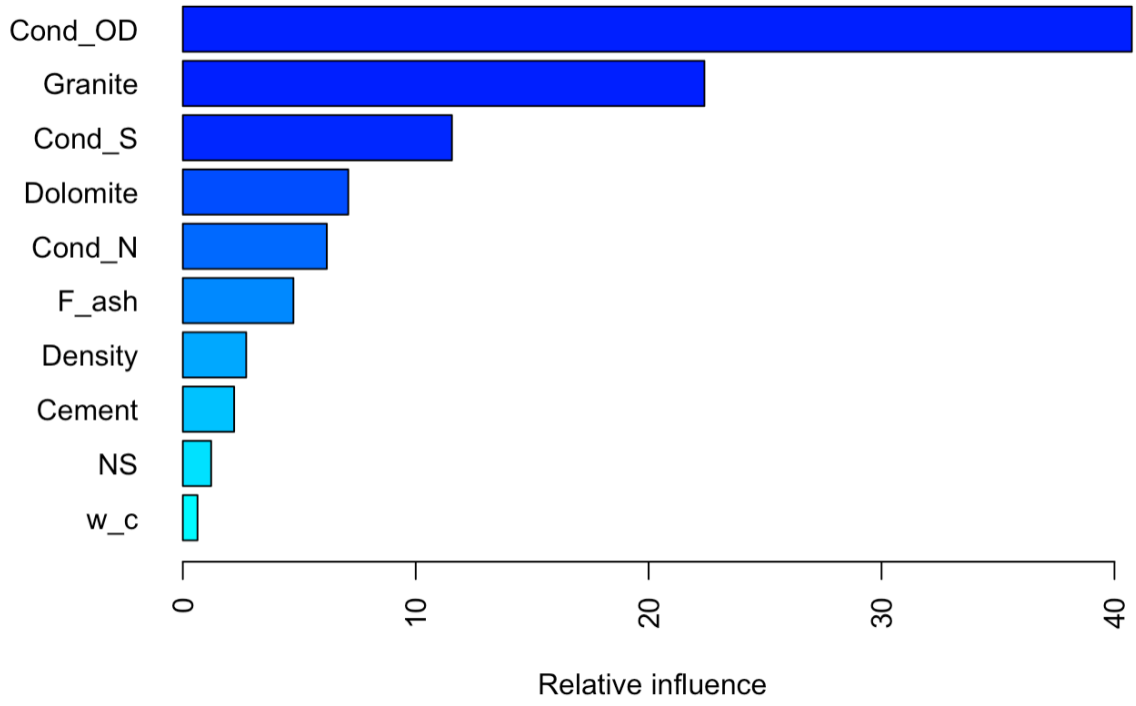

Figure 27. Concrete Constituent Relevance for Thermal Conductivity

The model provided competent results. The moisture conditions were instrumental in the estimation of an accurate thermal conductivity. This relative influence validated previous research on this thermal property and the lab-tested data obtained in this project. Higher moisture conditions are associated with a higher thermal conductivity value and established a prominent role in the estimation process. Aggregate type proved to play a critical role in impacting thermal conductivity. The data contained in Table 28, as well as the trends displayed in Figure 14, both illustrated a trend in aggregate type. Concrete Mixtures 8 (605/20.66FA/0.43/12.09D/5.0) and 10 (590/18.64FA/0.439/10.87D/5.9) resulted in higher thermal conductivity values compared to similar mixtures due to the mixtures composition of dolomite. Dolomite has been proven to

provide higher thermal property values, and this machine learning application technique validated the impact of the material. As expected, fly ash and density displayed crucial roles in thermal conductivity prediction. This study could not clearly depict the common trend of larger fly ash replacement percentages resulting in lower thermal conductivities due to the twelve selected mixtures containing similar replacement percentages. However, concrete mixtures containing a higher fly ash replacement percentage result in a less dense mixture, which was proven to play a crucial role in thermal conductivity. This model validated the relationship between density and thermal conductivity provided in Figure 14.

The machine learning technique was similarly used to investigate the variable importance of concrete mixtures in CTE lab tested results. Aggregate and fly ash types have proven to play a crucial role in impacting concrete mixtures CTE results. These predictions were validated by the machine learning technique and are displayed in Figure 28.

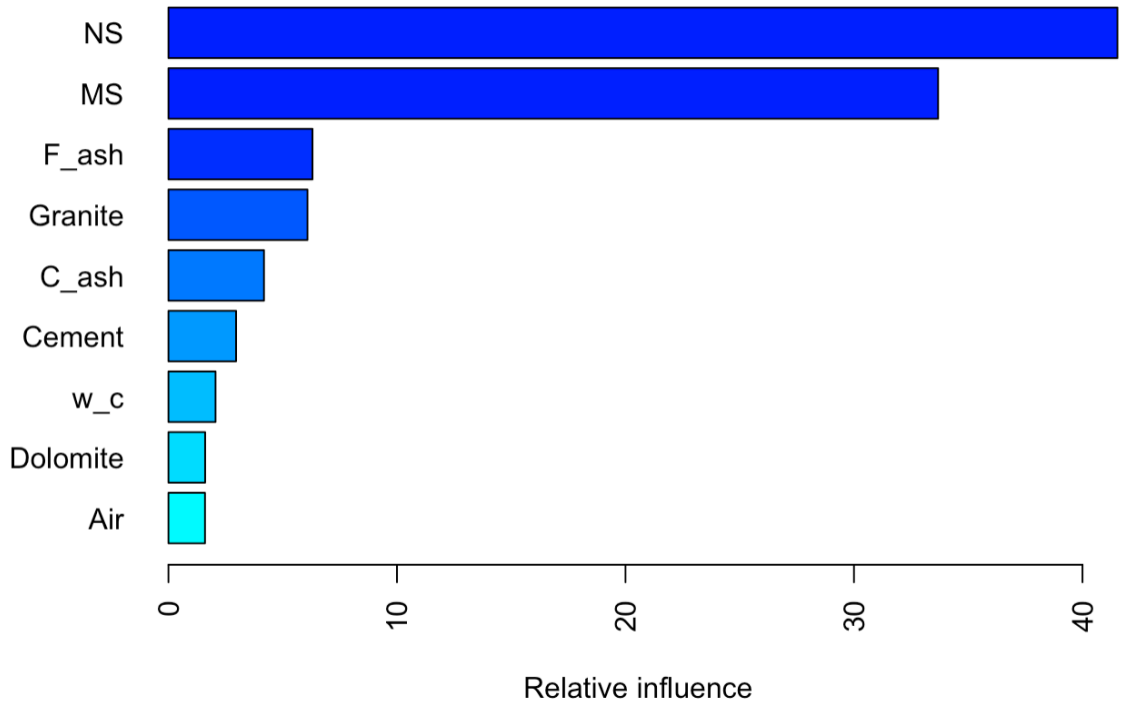

Figure 28. Concrete Constituent Relevance for CTE

Aggregate type played an expected role in the CTE prediction process. The study conducted by Kim (2014), summarized in Table 32, concluded similar variable importance. These results are expected due to the large volume of the concrete mixture comprising of the coarse and fine aggregates. Natural sand (NS) was previously proven to yield higher CTE values than similar mixtures containing manufactured sand (MS). This relationship between these two types of fine aggregate played a clear role in the prediction process. Along with fine aggregate, coarse aggregate illustrated a vital part in the CTE prediction process. The results in this study highlighted the impact that the different coarse aggregate types, including dolomite and granite, had on the thermal properties of concrete mixtures. The GBM for CTE endorsed the importance of coarse aggregate type as a concrete mixture input impacting thermal properties. Fly ash exemplified significance in CTE prediction as well. The different types of fly ash, class C-fly ash and class F-fly, were previously proven to impact CTE. A study conducted by Kim et al. (2015) established that concrete mixtures containing class C-fly ash contained significantly higher CTE values than similar mixtures containing class F-fly ash. This model verified the importance of the different types of this admixture, and its impact on the concrete's coefficient of thermal expansion.

9.0 CONCLUSIONS AND RECOMMENDATIONS

This project developed many important conclusions from testing the twelve GDOT approved mixtures while also exploring the relevance of property inputs through sensitivity analyses and machine learning applications. Some of the conclusions drawn from the lab tested data include:

- The large beam MOR testing conducted during this project validated the MOR results established by Wing (2018) in the development of the mechanical properties database. The 28-day MOR values range from 620 to 805 psi (4.3 to 5.6 MPa), and the 90-day MOR values range from 665 to 755 psi (4.6 to 5.2 MPa).
- Aggregate type was identified as the leading factor contributing to the coefficient of thermal expansion values. Concrete mixtures containing the dolomite aggregate type resulted in higher CTE values than similar mixtures containing granite aggregate type.
- For thermal conductivity, several conclusions were established:
    - The density of the concrete mixture largely impacted the thermal property.
    - A higher density results in a higher thermal conductivity value.
    - Moisture also plays an important role in thermal conductivity test values; specimens with a higher moisture content resulted in a higher thermal conductivity value.
    - Similar to CTE, mixtures containing the dolomite aggregate type exhibited higher thermal conductivity values than similar mixtures containing granite.
- A relationship between CTE and thermal conductivity was established. It is attributed to concrete mixtures containing lower thermal conductivity values serve as a better thermal buffer than mixtures with high thermal conductivity test results. Figure 15 illustrated this

relationship and can be utilized to estimate a thermal conductivity value during the MEPDG approach when a lab-tested thermal conductivity value is not readily available.

- During the sensitivity analyses CTE demonstrated itself to be the most critical thermal property for all pavement predictions concerning Pavement ME software.
- The machine learning application demonstrated several important trends in the various concrete mixture inputs impacting thermal properties.
    - Thermal conductivity: Moisture proved to play an important role in the prediction of this thermal property. The model validated the lab tested data that demonstrated an increase in moisture increased thermal conductivity values. Aggregate type also displayed an important impact and confirmed the test results that concluded dolomite provided higher thermal conductivity values than similar mixtures that contained granite. Fly ash and density both had a large impact on predicting the thermal conductivity and confirmed previous studies that stated the relevance of these factors.
    - Coefficient of thermal expansion: Aggregate type proved to be the controlling variables in the prediction of CTE. Both fine and coarse aggregates impacted the thermal property. The model validated previous research that concluded the various fine and coarse aggregate types were the leading factors affecting CTE. Fly ash type also proved to be important and verified a previous study in Georgia that highlighted different admixture types' relevance.

It is recommended that the measurement and investigation of ultimate shrinkage continue to understand the factors impacting the property fully.

REFERENCES

AASHTO, “Standard Test Method for the Coefficient of Thermal Expansion of Hydraulic Cement Concrete (T336-11)”, 2011.

ARA, A. R. A. (2015). *Implementation of the Mechanistic-Empirical Pavement Design Guide in Georgia*. (FHWA-GA-14-11-17).

Barone, Adam. “How Residual Sum of Squares (RSS) Works.” *Investopedia*, Investopedia, 28 Aug. 2020

B. Boukhatem, S. Kenai, A. Tagnit-Hamou, and M. Ghrici, “Application of new information technology on concrete: an overview/nauju˛ informaciniu˛ technologiju˛ naudojimas ruoˇsiant betona˛. Apzvalga,” ˇ Journal of Civil Engineering and Management, vol. 17, no. 2, pp. 248–258, 2011.

Bentz, D.P., Peltz, M.A., Duran-Herrera, A., Valdez, P., Juarez, C.A. 2011. *Thermal properties of high-volume fly ash mortars and concretes*. Journal of Building Physics. 34(3): 263-275.

Boehmke, Bradley. “Gradient Boosting Machines.” *Gradient Boosting Machines · UC Business Analytics R Programming Guide*, 14 June 2018, uc-r.github.io/gbm_regression.

Chintakunta, S. (2007). Sensitivity of thermal properties of pavement materials using mechanistic-empirical pavement design guide. MS Thesis. Iowa State University, Ames, Iowa.

Cihan, M. Timur. “Prediction of Concrete Compressive Strength and Slump by Machine Learning Methods.” *Advances in Civil Engineering*, vol. 2019, 2019, pp. 1–11., doi:10.1155/2019/3069046.

D. C. Montgomery, Design and Analysis of Experiments, John Wiley & Sons, Hoboken, NJ, USA, 2017.

dos Santos, W. N. (2003). Effect of moisture and porosity on the thermal properties of a conventional refractory concrete. *Journal of the European Ceramic Society*, *23*(5), 745–755. https://doi.org/10.1016/S0955-2219(02)00158-9

Kim, S.-H. (2012). *Determination of Coefficient of Thermal Expansion for Portland Cement* (10-04). Retrieved from Marietta, GA:

Kim, S.-H. (2014). "COMPARISON OF ARTIFICIAL NEURAL NETWORK AND RESPONSE SURFACE MODEL FOR ESTIMATING THE COEFFICIENT OF THERMAL EXPANSION OF CONCRETE MIXTURE ".

Kim, S.-H., et al. (2015). "Effect of materials and age on the coefficient of thermal expansion of concrete paving mixture." Road Materials and Pavement Design 16(2): 445-458.

Kodide, U. (2010). *Thermal Conductivity and its Effects on the Performance of PCC Pavements in MEPDG.* (Masters of Science in Civil Engineering), Louisiana State University.

L. Breiman, "Bagging predictors," *Machine Learning*, vol. 24, no. 2, pp. 123–140, 1996.

Mallela, J., Abbas, A., Harman, T., Rao, C. T., Liu, R. F., Darter, M. I., & Trb. (2005). Measurement and significance of the coefficient of thermal expansion of concrete in rigid pavement design *Rigid and Flexible Pavement Design 2005* (pp. 38-46). Washington: Transportation Research Board Natl Research Council.

M. Hofmann and R. Klinkenberg, RapidMiner: Data Mining Use Cases and Business Analytics Applications, CRC Press, Boca Raton, FL, USA, 2013.

P. Chopra, R. K. Sharma, M. Kumar, and T. Chopra, “Comparison of machine learning techniques for the prediction of compressive strength of concrete,” Advances in Civil Engineering, vol. 2018, Article ID 5481705, 9 pages, 2018.

Shin, A. H. C., & Kodide, U. (2012). Thermal conductivity of ternary mixtures for concrete pavements. *Cement & Concrete Composites,* 34(4), 575-582.

Yang, J. and S.-H. Kim (2014). "Factorial effects of mix design variables on the coefficient of thermal expansion of concrete mixtures." Road Materials and Pavement Design 15(4): 942-952.

Kim, S.-H. (2014). "COMPARISON OF ARTIFICIAL NEURAL NETWORK AND RESPONSE SURFACE MODEL FOR ESTIMATING THE COEFFICIENT OF THERMAL EXPANSION OF CONCRETE MIXTURE ".

Kim, S.-H., et al. (2015). "Effect of materials and age on the coefficient of thermal expansion of concrete paving mixture." Road Materials and Pavement Design **16**(2): 445-458.

Kim, S., Worthey, H.; Brink, W., Von Quintus, H., Durham, S., Chorzepa, M. (2020), “Development of Innovative & Effective Training Modules and Methods for Pavement Designers for Rapid Deployment and Continuous Operation of MEPDG”, GDOT RP 17-18 Final Report

“QPL Requirements.” *Materials*, www.dot.ga.gov/PS/Materials/QPLRequirements.

Quintus, H. V. L., Darter, M. I., Bhattacharya, B. B., & Titus-Glover, L. (2015). *Implementation and Calibration of the MEPDG in Georgia Task Order 3 Final Report* (FHWA/GA-014-11-17).

Tanesi, J., Kutay, M. E., Abbas, A., & Meininger, R. (2007). Effect of Coefficient of Thermal Expansion Test Variability on Concrete Pavement Performance as Predicted by Mechanistic-Empirical Pavement Design Guide. *Transportation Research Record*, *2020*(1), 40–44

Wing, D. (2018). Development of Concrete Mechanical Properties Database for Pavement Mechanistic-Emperical Input. MS Thesis. University of Georgia, Athens, Georgia.

Yang, J. and S.-H. Kim (2014). "Factorial effects of mix design variables on the coefficient of thermal expansion of concrete mixtures." Road Materials and Pavement Design 15(4): 942-952.

Y. Song and Y. Lu, “Decision tree methods: applications for classification and prediction,” *Shanghai Archives of Psychiatry*, vol. 27, no. 2, pp. 130–135, 2015

APPENDICES

Trial 1 Fresh Property Test Results

Mixture	Temperature (◦F)	Slump (in)	Air (%)	Unit Weight (lb/ft3)
1	83.0	0.50	4.9	147.2
2	83.4	2.25	4.0	147.4
3	72.4	3.00	6.2	144.4
4	72.7	8.50	6.1	143.0
5	71.2	7.00	4.5	143.4
6	74.1	6.50	5.5	141.6
7	70.0	4.25	3.1	145.2
8	68.4	5.00	5	148.8
9	74.0	0.50	4.9	145.8
10	69.7	2.50	5.9	147.2
11	70.5	2.75	3.6	146.6
12	77.0	2.75	4.7	146.4

Trial 2 Fresh Property Test Results

Mixture	Temperature (◦F)	Slump (in)	Air (%)	Unit Weight (lb/ft3)
1	80.0	1.0	4.0	150.0
2	82.0	2.0	3.1	147.6
3	78.0	1.0	5.1	147.8
4	80.0	2.5	4.9	145.4
5	78.6	0.5	4.1	144.8
6	80.9	1.5	4.0	143.8
7	79.0	2.0	3.2	146.4
8	79.0	1.5	3.3	149.4
9	82.0	1.5	5.1	143.6
10	80.0	2.0	5.2	146.8
11	80.0	2.0	3.5	147.4
12	81.0	3.0	5.1	146.1

Trial 3 Fresh Property Test Results

Mixture	Temperature (◦F)	Slump (in)	Air (%)	Unit Weight (lb/ft3)
1	64.0	0.5	4.1	149.4
2	64.0	1.5	3.5	150.4
3	67.0	0.5	3.6	150.4
4	73.0	2.5	4.7	148.2
5	81.0	0.5	4.2	145.0
6	80.0	1.3	3.8	144.8
7	76.0	2.5	2.4	147.8
8	76.0	1.5	3.3	151.0
9	78.8	1.0	4.5	143.0
10	72.0	1.5	5.4	149.4
11	75.0	2.0	3.1	148.8
12	76.0	2.5	4.4	147.8

Vulcan Materials Company

Stockbridge
3925 North Henry Blvd
Stockbridge, GA 30281
678-229-7885

05/06/2019

570-#57 (25290)

Procedure	Sieve/Test	Average	Unit	GADOT 57
	1 1/2" (37.5mm)	100.0	%	100.0-100.0
	1" (25mm)	98.3	%	95.0-100.0
	3/4" (19mm)	83.3	%	
	1/2" (12.5mm)	37.2	%	25.0-60.0
	3/8" (9.5mm)	16.5	%	
	#4 (4.75mm)	1.4	%	0.0-10.0
	#8 (2.36mm)	0.6	%	0.0-5.0
	#200 (75µm)	0.00	%	
	LA Abrasion (B,500)	46	%	0-50
	FM	6.96		
	SE	57	%	
	Absorption	0.6	%	
	Total Moisture	1.02	%	
	SPGR (Dry,Gsb)	2.609		
	SPGR (SSD)	2.625		
	SPGR (Apparent,Gsa)	2.652		
	Unit Wt (Loose)	90	lb/ft3	
	Unit Wt (Rodded)	97	lb/ft3	

Vulcan Materials Company

Kennesaw
1272 Duncan Road
Kennesaw, GA 30144
770-427-2401

05/06/2019

570-#57 (25290)

Procedure	Sieve/Test	Average	Unit	ASTM 57
	1 1/2" (37.5mm)	100.0	%	100.0-100.0
	1" (25mm)	97.1	%	95.0-100.0
	3/4" (19mm)	83.8	%	
	1/2" (12.5mm)	37.1	%	25.0-60.0
	3/8" (9.5mm)	16.7	%	
	#4 (4.75mm)	2.6	%	0.0-10.0
	#8 (2.36mm)	1.4	%	0.0-5.0
	#200 (75µm)	0.00	%	
	LA Abrasion (B,500)	41.8		
	Wash Loss (#200/75um)	0.5	%	
	Absorption	0.65		
	Total Moisture	1.31	%	
	SPGR (Dry,Gsb)	2.745		
	SPGR (SSD)	2.763		
	SPGR (Apparent,Gsa)	2.795		
	Unit Wt (Loose)	100.3	lb/ft3	
	Unit Wt (Rodded)	108.7	lb/ft3	

Vulcan Materials Company

Adairsville
292 E Mitchell Road
Adairsville, GA 30103
770-773-3217

05/06/2019

570-#57 (25291)

Procedure	Sieve/Test	Average	Unit	GADOT 57
	2" (50mm)	100.0	%	
	1 1/2" (37.5mm)	100.0	%	100.0-100.0
	1" (25mm)	99.4	%	95.0-100.0
	3/4" (19mm)	84.5	%	
	1/2" (12.5mm)	41.5	%	25.0-60.0
	3/8" (9.5mm)	17.5	%	
	#4 (4.75mm)	1.5	%	0.0-10.0
	#8 (2.36mm)	0.6	%	0.0-5.0
	#200 (75µm)	0.00	%	0.00-1.50
	LA Abrasion (B,500)	18	%	0-60
	Flat/Elongated (5:1)	0.85	%	
	-#200 (75um)	0.24	%	
	Absorption	0.08	%	
	Total Moisture	0.51	%	
	SPGR (Dry,Gsb)	2.846		
	SPGR (SSD)	2.847		
	SPGR (Apparent,Gsa)	2.851		
	Unit Wt (Loose)	96	lb/ft3	
	Unit Wt (Rodded)	104	lb/ft3	

Martin Marietta

Basic Quality Statistical Summary Report

Plant 21209-Ruby Quarry
Product 0570-GDOT #57 Stone
Specification GADOT 57
Period 01/01/2019 - 05/06/2019

Sieve/Test	Tests	Average	St Dev	Target	Specification
1 1/2" (37.5mm)	163	100.0	0.00	100-100	100-100
1" (25mm)	163	98.5	0.80	97-100	95-100
3/4" (19mm)	163	85.7	3.88		
1/2" (12.5mm)	163	42.5	4.37	32-48	25-60
3/8" (9.5mm)	163	20.4	3.28		
#4 (4.75mm)	163	1.1	0.55	0-5	0-10
#8 (2.36mm)	163	0.1	0.21	0-2	0-5
#200 (75µm)	1	0.10			
Pan	163	0.00	0.000		

Query Query Selections
Date Created 05/06/2019
Date Range 01/01/2019 - 05/06/2019
Plant Ruby Quarry

Atlanta Sand & Supply Company

Detail Quality Statistical Summary Report

Plant 01-Burke Pit
Product 2 B-Burke Concrete Sand
Specification 2 B Burke Concrete Sand
Period 05/06/2019 - 05/10/2019

Sieve/Test	Tests	Average	Min	Max	Range	St Dev	Target	Specification	PWS
3/8" (9.5mm)	5	100	100	100	0	0.0		100-100	100.0
#4 (4.75mm)	5	100	100	100	0	0.0		95-100	100.0
#8 (2.36mm)	5	99	98	99	1	0.4			
#16 (1.18mm)	5	90	87	91	4	1.5		45-95	100.0
#30 (0.6mm)	5	60	55	61	6	2.6			
#50 (0.3mm)	5	21	19	23	4	1.8		8-30	100.0
#100 (0.15mm)	5	2	1	4	3	1.3		0-10	100.0
Pan	5	0.0	0.0	0.0	0.0	0.00			
FM	5	2.297	2.262	2.385	0.123	0.0499			
SE	2	93.500	91.000	96.000	5.000	3.5355			
Wash Loss (#200/75um)	1	0.418	0.418	0.418	0.000				

Query Query Selections
Date Created 05/10/2019
Date Range 05/06/2019 - 05/10/2019
Plant Burke Pit
Sample Type Shipping

ARGOS

Cement Mill Test Report

Month of Issue: April 2019

Plant:	Calera, AL
Product:	Portland Cement Type I
Silo:	17, 18J, 19, 20
Manufactured:	March 2019

ASTM C150 and AASHTO M85 Standard Requirements

CHEMICAL ANALYSIS

Item	Spec limit	Test Result
Rapid Method, X-Ray *(C114)*		
SiO2 (%)	---	19.8
Al2O3 (%)	---	4.7
Fe2O3 (%)	---	3.2
CaO (%)	---	62.8
MgO (%)	6.0 max	3.0
SO3 (%)	3.0 max *	3.0
Loss on Ignition (%)**	3.5 max	2.7
Insoluble residue (%)	1.5 max	0.51
CO2 (%)	---	1.7
Limestone (%)	5.0 max	2.3
CaCO3 in Limestone (%)	70 min	99
Inorganic Process Addition (Baghouse Dust)	5.0 max	2.0
Adjusted Potential Phase Composition *(C150)*		
C3S (%)	---	54
C2S (%)	---	15
C3A (%)	---	7
C4AF (%)	---	10
ASTM C150 and AASHTO M85 Optional Chemical Requirements:		
NaEq (%)	0.60 max	0.36

PHYSICAL ANALYSIS

Item	Spec limit	Test Result	
Air content of mortar (%) *(C185)*	12 max	7	
Blaine Fineness (m^2/kg) *(C204)*	260	396	
-325 (%) *(C430)*	---	97.2	
Autoclave expansion (%) *(C151)*	0.80 max	0.08	
Compressive strength (MPa, [PSI]) *(C109)*			
1 day		14.4	[2090]
3 days	12.0 [1740] min	27.0	[3910]
7 days	19.0 [2760] min	33.7	[4890]
28 days (Reflects previous month's data)	---	44.3	[6420]
Time of setting (minutes)			
Vicat Initial *(C191)*	45 - 375	101	
Heat of Hydration (kJ/kg) (C1702)			
3 days (for information only)***	---	298	
Mortar Bar Expansion (%) (C1038)***	0.020 max	0.003	
Density (C188)		3.13	

* May exceed 3.0% SO3 maximum based on our C1038 results of < 0.020% expansion at 14 days.

** Loss on ignition max of 3.5% when limestone is an ingredient

*** Test result represents most recent value and is provided for information only.

We certify that the above described cement, at the time of shipment, meets the chemical and physical requirements of applicable FDOT Section 921, ALDOT, GDOT, TDOT, MDOT, INDOT, La DOTD, NCDOT, ODOT, PennDOT, VDOT, SCDOT, AHTD Specifications for TYPE I;
ASTM C150 & AASHTO M85 STANDARD SPECIFICATIONS FOR TYPE I CEMENT;
ASTM C150 & AASHTO M85 OPTIONAL CHEMICAL REQUIREMENTS FOR TYPE I LOW ALKALI CEMENT.

Certified By:

Nicholas T. Ewing - Quality Coordinator

Argos USA - Roberta
8039 Highway 25, Calera, AL 35040
Phone: 205.668.2721

Report created: 04/17/2019

BORAL RESOURCES

Materials Testing & Research Facility
2650 Old State Hwy 113
Taylorsville, GA 30178
770-684-0102

ASTM C618 / AASHTO M295 Testing of Bowen Fly Ash

Sample Date: 10/1 - 10/31/18 **Report Date:** 12/13/2018

Sample Type: Monthly **MTRF ID:** 3146BN

Sample ID:

Chemical Analysis	Results	ASTM Limit Class F/C	AASHTO Limit Class F/C
Silicon Dioxide (SiO2)	47.49 %		
Aluminum Oxide (Al2O3)	21.30 %		
Iron Oxide (Fe2O3)	18.08 %		
Sum (SiO2+Al2O3+Fe2O3)	86.87 %	70.0/50.0 min	70.0/50.0 min
Sulfur Trioxide (SO3)	2.07 %	5.0 max	5.0 max
Calcium Oxide (CaO)	4.26 %		
Magnesium Oxide (MgO)	1.19 %		
Sodium Oxide (Na2O)	0.99 %		
Potassium Oxide (K2O)	2.32 %		
Sodium Oxide Equivalent (Na2O+0.658K2O)	2.52 %		
Moisture	0.14 %	3.0 max	3.0 max
Loss on Ignition	1.23 %	6.0 max	5.0 max
Available Alkalies, as Na2Oe	1.03 %	Not Required	1.5 max* *when required by purchaser
Physical Analysis			
Fineness, % retained on 45-µm sieve	14.48 %	34 max	34 max
Strength Activity Index - 7 or 28 day requirement			
7 day, % of control	82 %	75 min	75 min
28 day, % of control	82 %	75 min	75 min
Water Requirement, % control	98 %	105 max	105 max
Autoclave Soundness	0.01 %	0.8 max	0.8 max
Density	2.47		

The test data listed herein was generated by applicable ASTM methods. The reported results pertain only to the sample(s) or lot(s) tested. This report cannot be reproduced without permission from Boral Resources.

Doug Rhodes, CET
Facility Manager

AASHTO ACCREDITED